

1 **Plant responses to volcanically-elevated CO<sub>2</sub> in two Costa Rican**  
2 **forests**

3 Robert R. Bogue<sup>1,2,3</sup>, Florian M. Schwandner<sup>1,4</sup>, Joshua B. Fisher<sup>1</sup>, Ryan Pavlick<sup>1</sup>, Troy S.  
4 Magney<sup>1</sup>, Caroline A. Famiglietti<sup>1</sup>, Kerry Cawse-Nicholson<sup>1</sup>, Vineet Yadav<sup>1</sup>, Justin P. Linick<sup>1</sup>,  
5 Gretchen B. North<sup>6</sup>, Eliecer Duarte<sup>7</sup>

6 <sup>1</sup>Jet Propulsion Laboratory, California Institute of Technology, 4800 Oak Grove Drive, Pasadena, CA 91109, USA

7 <sup>2</sup>Geology Department, Occidental College, 1600 Campus Road, Los Angeles, CA 90041, USA

8 <sup>3</sup>Department of Earth and Planetary Sciences, McGill University, 845 Sherbrooke St W, Montréal, QC H3A 0G4,  
9 CA

10 <sup>4</sup>Joint Institute for Regional Earth System Science and Engineering, University of California Los Angeles, Los  
11 Angeles, CA 90095

12 <sup>5</sup>Department of Earth System Science, Stanford University, 450 Serra Mall, Stanford, CA 94305, USA

13 <sup>4</sup>Biology Department, Occidental College, 1600 Campus Road, Los Angeles, CA 90041, USA

14 <sup>5</sup>Observatory of Volcanology and Seismology (OVSICORI), Universidad Nacional de Costa Rica, 2386-3000  
15 Heredia, Costa Rica

16 *Correspondence to:* Florian M. Schwandner (Florian.Schwandner@jpl.caltech.edu)

17

18

19

Revised manuscript prepared for:

20

Biogeosciences (Copernicus), <https://www.biogeosciences.net/>

21

REV3 (2019-02-17)

22

23 **Abstract.** We explore the use of active volcanoes to determine the short- and long-term effects of elevated CO<sub>2</sub> on  
24 tropical trees. Active volcanoes continuously but variably emit CO<sub>2</sub> through diffuse emissions on their flanks,  
25 exposing the overlying ecosystems to elevated levels of atmospheric CO<sub>2</sub>. We found tight correlations ( $r^2=0.86$  and  
26  $r^2=0.74$ ) between wood stable carbon isotopic composition and co-located volcanogenic CO<sub>2</sub> emissions for two of  
27 three investigated species (*Oreopanax xalapensis* and *Buddleja nitida*), which documents the long-term  
28 photosynthetic incorporation of isotopically heavy volcanogenic carbon into wood biomass. Measurements of leaf  
29 fluorescence and chlorophyll concentration suggest that volcanic CO<sub>2</sub> also has measurable short-term functional  
30 impacts on select species of tropical trees. Our findings indicate significant potential for future studies to utilize  
31 ecosystems located on active volcanoes as natural experiments to examine the ecological impacts of elevated  
32 atmospheric CO<sub>2</sub> in the tropics and elsewhere. Results also point the way toward a possible future utilization of  
33 ecosystems exposed to volcanically elevated CO<sub>2</sub> to detect changes in deep volcanic degassing by using selected  
34 species of trees as sensors.

## 35 **1 Introduction**

36 Tropical forests represent about 40% of terrestrial Net Primary Productivity (NPP) worldwide, store 25% of biomass  
37 carbon, and may contain 50% of all species on Earth, but the projected future responses of tropical plants to globally  
38 rising levels of CO<sub>2</sub> are poorly understood (Leigh et al., 2004; Townsend et al., 2011). The largest source of uncertainty  
39 comes from a lack of understanding of long-term CO<sub>2</sub> fertilization effects in the tropics (Cox et al., 2013). Reducing  
40 this uncertainty would significantly improve Earth system models, advances in which would help better constrain  
41 projections in future climate models (Cox et al., 2013; Friedlingstein et al., 2013). Ongoing debate surrounds the  
42 question of how much more atmospheric CO<sub>2</sub> tropical ecosystems can absorb—the “CO<sub>2</sub> fertilization effect” (Gregory  
43 et al., 2009; Kauwe et al., 2016; Keeling, 1973; Schimel et al., 2015).

44 Free Air CO<sub>2</sub> Enrichment (FACE) experiments have been conducted to probe this question, but none have  
45 been conducted in tropical ecosystems (e.g. Ainsworth and Long, 2005; Norby et al., 2016). Some studies have used  
46 CO<sub>2</sub>-emitting natural springs to study plant responses to elevated CO<sub>2</sub>, but these have been limited in scope due to the  
47 small spatial areas around springs that experience elevated CO<sub>2</sub> (Hattenschwiler et al., 1997; Körner and Miglietta,  
48 1994; Paoletti et al., 2007; Saurer et al., 2003). These studies have suffered from several confounding influences,  
49 including other gas species that accompany CO<sub>2</sub> emissions at these springs, human disturbances, and difficulty with  
50 finding appropriate control locations. Additionally, none have been conducted in the tropics (Pinkard et al., 2010). A  
51 series of studies in Yellowstone National Park (USA) used its widespread volcanic hydrothermal CO<sub>2</sub> emissions for  
52 the same purpose, though it is not in the tropics (Sharma and Williams, 2009; Tercek et al., 2008). Yellowstone was  
53 particularly suitable for this type of study, due to its protected status as a National Park, and because the large areas  
54 of CO<sub>2</sub> emissions made control points more available (Sharma and Williams, 2009; Tercek et al., 2008). These studies  
55 reported changes in rubisco, an enzyme central to CO<sub>2</sub> fixation, and sugar production in leaves similar to results from  
56 FACE experiments, suggesting that volcanically-influenced areas like Yellowstone have untapped potential for  
57 studying the long-term effects of elevated CO<sub>2</sub> on plants.

58 Tropical ecosystems on the vegetated flanks of active volcanoes offer large and diverse ecosystems that could  
59 make this type of study viable. Well over 200 active volcanoes are in the tropics (Global Volcanism Program, 2013)  
60 and many of these volcanoes are heavily forested. However, fewer of these tropical volcanic forests have sufficient  
61 legal protection to be a source of long-term information, and the effects of diffuse volcanic flank gas emissions on the  
62 overlying ecosystems remain largely unknown. Most previous studies focused on extreme conditions, such as tree kill  
63 areas associated with extraordinarily high CO<sub>2</sub> emissions at Mammoth Mountain, CA (USA) (Biondi and Fessenden,  
64 1999; Farrar et al., 1995; Sorey et al., 1998). However, the non-lethal effects of cold volcanic CO<sub>2</sub> emissions—away  
65 from the peak emission zones, but still in the theorized fertilization window—have received little attention, and could  
66 offer a new approach to studying the effects of elevated CO<sub>2</sub> on ecosystems (Cawse-Nicholson et al., 2018; Vodnik  
67 et al., 2018). The broad flanks of active volcanoes experience diffuse emissions of excess CO<sub>2</sub> because the underlying  
68 active magma bodies continuously release gas, dominated by CO<sub>2</sub> transported to the surface along fault lines (Chiodini  
69 et al., 1998; Dietrich et al., 2016; Farrar et al., 1995). This process has frequently been studied to understand the  
70 dynamics of active magma chambers and to assess potential volcanic hazards (Chiodini et al., 1998; Sorey et al.,  
71 1998). These emissions are released through faults and fractures on the flanks of the volcano (Burton et al., 2013;  
72 Pérez et al., 2011; Williams-Jones et al., 2000)(see Supplementary Figure S1). Volcanic flanks through which these  
73 gases emanate are broad, covering typically 50-200 km<sup>2</sup>, often supporting well-developed, healthy ecosystems. Some  
74 of these faults tap into shallow acid hydrothermal aquifers, but by the time these gases reach the surface of most  
75 forested volcanoes, soluble and reactive volcanic gas species (e.g., SO<sub>2</sub>, HF, HCl, H<sub>2</sub>S) have been scrubbed out in the  
76 deep subsurface, leading to a diffusely emanated gas mix of predominantly CO<sub>2</sub> with minor amounts of hydrogen,  
77 helium, and water vapor reaching the surface (Symonds et al., 2001).

78 Trees in these locations are continuously exposed to somewhat variably elevated concentrations of CO<sub>2</sub>  
79 (eCO<sub>2</sub>), although the specific effects of this eCO<sub>2</sub> on the trees are not well understood. Volcanic CO<sub>2</sub> has no <sup>14</sup>C and  
80 a δ<sup>13</sup>C signature typically ranging from around -7 to -1 ‰, which is distinct from typical vegetation and noticeably  
81 enriched in <sup>13</sup>C compared to typical atmospheric values (Mason et al., 2017). If trees incorporate volcanic CO<sub>2</sub>, then  
82 the stable carbon isotopic composition of wood may document the long-term, possibly variable influence of volcanic  
83 CO<sub>2</sub> during the tree's growth. With this tracer available, volcanic ecosystems could become a valuable natural  
84 laboratory to study the long-term effects of elevated CO<sub>2</sub> on ecosystems, especially in understudied regions like the  
85 tropics. Several studies have found correlations between variations in volcanic CO<sub>2</sub> flux and plant <sup>14</sup>C records at  
86 Mammoth Mountain, Yellowstone, and Naples which agreed well with previous observations at these well-studied  
87 sites (Cook et al., 2001; Evans et al., 2010; Lefevre et al., 2017; Lewicki et al., 2014). The Mammoth Mountain and  
88 Yellowstone studies linked seismic swarms and accompanying increases in CO<sub>2</sub> flux to decreases in <sup>14</sup>C content in  
89 tree rings in 1 or 2 trees, demonstrating the methods utility for uncovering yearly-scale variations in volcanic CO<sub>2</sub>  
90 fluxes (Cook et al., 2001; Evans et al., 2010; Lewicki et al., 2014). The Naples study instead focused on using <sup>14</sup>C in  
91 grasses as short term (2 to 6 month) monitors of volcanic CO<sub>2</sub> flux, which is useful for volcanic monitoring due to the  
92 time-integrated signal they provide (Lefevre et al., 2017). A study of plants growing at Furnas volcano found very  
93 strong (r<sup>2</sup>>0.85) correlations between depletions in <sup>14</sup>C and enrichments in <sup>13</sup>C from volcanic CO<sub>2</sub> in three species of  
94 plants, although this study also had a relatively limited (5 samples per species) dataset (Pasquier-Cardin et al., 1999).

95 The previously mentioned Naples study also found some correlation between  $^{13}\text{C}$  and  $^{14}\text{C}$ , although it was not as strong  
96 as the study in Furnas (Lefevre et al., 2017; Pasquier-Cardin et al., 1999). Additionally, short-term effects of  $\text{eCO}_2$   
97 might be revealed by plant functional measurements at the leaf scale, where the additional  $\text{CO}_2$  could increase carbon  
98 uptake in photosynthesis. A series of studies at Mt. Etna in Italy and Mt. Nyiragongo in the Democratic Republic of  
99 the Congo found linear anomalies in NDVI (normalized difference vegetation index), a measure of vegetation  
100 greenness (Houlié et al., 2006). One to two years after the appearance of the NDVI anomalies, flank eruptions occurred  
101 directly along the line of the anomaly, indicating a plant response to the volcano's pre-eruptive state which may be  
102 due to increased  $\text{CO}_2$  emissions in the buildup to the eruption (Houlié et al., 2006). A follow-up study found that the  
103 trees on Mt. Etna were relatively insensitive to changes in temperature and water availability, strengthening the case  
104 that volcanic influence was indeed responsible for the NDVI anomaly (Seiler et al., 2017).

105 Here we provide preliminary results on the short- and long-term non-lethal impacts of diffuse volcanic  $\text{CO}_2$   
106 emissions on three species of tropical trees on the flanks of two active volcanoes in Costa Rica. We also explore the  
107 viability of studying volcanically-influenced ecosystems to better understand potential future responses to elevated  
108  $\text{CO}_2$  and suggest adjustments to our approach that will benefit future, similarly-motivated studies.

## 109 **2 Methods**

### 110 **2.1 Investigated locations and sampling strategy**

111 Irazú and Turrialba are two active volcanoes located ~25 and 35 km east of San José, Costa Rica (Fig. 1). These two  
112 volcanoes are divided by a large erosional basin. The forested portions of the two volcanoes cover approximately 315  
113  $\text{km}^2$ . The vast majority of the northern flanks of Irazú and Turrialba are covered in legally protected dense old-growth  
114 forest, while the southern flanks are dominated by pasture land and agriculture. Turrialba rises 3,300 m above its base  
115 and has been active for at least 75,000 years with mostly fumarolic activity since its last major eruption in 1866  
116 (Alvarado et al., 2006). It has experienced renewed activity beginning in 2010, and its current activity is primarily  
117 characterized by a near-constant volcanic degassing plume, episodic minor ash emissions, and fumarolic discharges  
118 at two of the summit craters, as well as significant diffuse and fumarolic gas emissions across its flanks, focused along  
119 fault systems (Martini et al., 2010). Turrialba's  $\text{CO}_2$  emissions in areas proximal to the crater were calculated at  
120  $\pm 46$  tons/d (Epiard et al., 2017). The Falla Ariete (Ariete fault), a major regional fault, runs northeast-southwest  
121 through the southern part of Turrialba's central edifice and is one of the largest areas of diffuse  $\text{CO}_2$  emissions on  
122 Turrialba (Epiard et al., 2017; Rizzo et al., 2016). Atmospheric  $\text{CO}_2$  has an average  $\delta^{13}\text{C}$  value of -9.2 ‰ at Turrialba,  
123 and the volcanic  $\text{CO}_2$  released at the Ariete fault has significantly heavier  $\delta^{13}\text{C}$  values clustered around -3.4 ‰  
124 (Malowany et al., 2017).

125 Irazú has been active for at least 3,000 years and had minor phreato-magmatic eruptions in 1963 and a single  
126 hydrothermal eruption in 1994. Currently, Irazú's activity primarily consists of shallow seismic swarms, fumarolic  
127 crater gas emissions, small volcanic landslides, and minor gas emissions on its northern forested flank (Alvarado et  
128 al., 2006; Barquero et al., 1995). Diffuse cold flank emissions of volcanic  $\text{CO}_2$  represent the vast majority of gas

129 discharge from Irazú, as the main crater releases 3.8 t d<sup>-1</sup> of CO<sub>2</sub> and a small area on the north flank alone releases 15  
130 t d<sup>-1</sup> (Epiard et al., 2017). Between the two volcanoes, a major erosional depression is partially occupied by extensive  
131 dairy farms and is somewhat less forested than their flanks.

132 In this study, we focused on accessible areas between 2,000 and 3,300 m on both volcanoes (Fig. 1). On  
133 Irazú, we sampled trees and CO<sub>2</sub> fluxes from the summit area to the north, near the approximately north-south striking  
134 Rio Sucio fault, crossing into the area dominated by dairy farms on Irazú's lower northeastern slope. Of significant  
135 importance for this type of study is that all active volcanoes on Earth continuously emit CO<sub>2</sub> diffusely through fractures  
136 and diffuse degassing structures on their flanks, at distances hundreds to thousands of meters away from the crater  
137 (Dietrich et al., 2016; Epiard et al., 2017), and this elevated CO<sub>2</sub> degassing persists continuously and consistently over  
138 decades to centuries (Burton et al., 2013; Delmelle and Stix, 1999; Nicholson, 2017). There is no inherent seasonal or  
139 meteorological variability of the source gas pressure, and no dependence on shallow soil or vegetation chemistry or  
140 biology (though increased soil moisture in the rainy season, wind, and atmospheric pressure can modulate gas  
141 permeability of the shallow soil) (Camarda et al., 2006). The soil overlying deep reaching fracture systems acts as a  
142 diffuser through which the volcanic gas percolates and enters the sub-canopy air. For our study sites, portions of the  
143 volcanoes with active "cold" CO<sub>2</sub> degassing have already been assessed and mapped previously (Epiard et al., 2017;  
144 Malowany et al., 2017).

145 Our sampling locations on Irazú were located along a road from the summit northward down into this low-  
146 lying area. On Turrialba, we focused on an area of known strong emissions but intact forests on the SW slope, uphill  
147 of the same erosional depression, but cross-cut by the major NE-SW trending active fracture system of the Falla Ariete.  
148 We sampled three main areas of the Falla Ariete, each approximately perpendicularly transecting the degassing fault  
149 along equal altitude; the upper Ariete fault, the lower Ariete fault, and a small basin directly east of the old Cerro  
150 Armado cinder cone on Turrialba's south-western flank. We took a total of 51 tree samples (17 were excluded after  
151 stress screening) at irregular intervals depending on the continued availability and specimen maturity of three species  
152 present throughout the transect.

153 All transects are in areas experiencing measurable CO<sub>2</sub> enhancements from the Falla Ariete, but not high  
154 enough in altitude to be in areas generally downwind of the prevailing crater emissions plume (Epiard et al., 2017).  
155 We avoided areas that experience ash fall, high volcanic SO<sub>2</sub> concentrations, local anthropogenic CO<sub>2</sub> from farms, or  
156 that were likely to have heavily acidified soil. Excessively high soil CO<sub>2</sub> concentrations can acidify soil, leading to  
157 negative impacts on ecosystems growing there (McGee and Gerlach, 1998). Because such effects reflect by-products  
158 of extreme soil CO<sub>2</sub> concentrations rather than direct consequences of elevated CO<sub>2</sub> on plants, we avoided areas with  
159 CO<sub>2</sub> fluxes high enough to possibly cause noticeable CO<sub>2</sub>-induced soil acidification. Light ash fall on some days likely  
160 derived from atmospheric drift, as we were not sampling in areas downwind of the crater. The ash fall did not in any  
161 noticeably way affect our samples, as trees showing ash accumulation on their leaves or previous damage were the  
162 exception and avoided. Altitude, amount of sunlight during measurements, and aspect had no consistent correlations  
163 with any of the parameters we measured.

## 164 2.2 Studied tree species

165 Our study focused on three tree species found commonly on Turrialba and Irazú: *Buddleja nitida*, *Alnus acuminata*,  
166 and *Oreopanax xalapensis*. *B. nitida* is a small tree with a typical stem diameter (DBH) ranging from 5 to 40 cm that  
167 grows at elevations of 2,000-4,000 m throughout most of Central America (Kappelle et al., 1996; Norman, 2000). The  
168 DBH of the individuals we measured ranged from 11.5 to 51.3 cm, with an average of 29.85 cm. It averages 4-15 m  
169 in height and grows primarily in early and late secondary forests (Kappelle et al., 1996; Norman, 2000). *A. acuminata*  
170 is a nitrogen-fixing pioneer species exotic to the tropics that can survive at elevations from 1,500-3,400 m, although  
171 it is most commonly found between 2,000-2,800 m (Weng et al., 2004). The trees we measured had DBH ranging  
172 from 14.3 to 112 cm, with an average of 57.14 cm. *O. xalapensis* thrives in early and late successional forests, although  
173 it can survive in primary forests as well (Kappelle et al., 1996; Quintana-Ascencio et al., 2004). It had the smallest  
174 average DBH of the three species, ranging from 6.6 to 40.9 cm, with an average of 22.71 cm.

## 175 2.3 CO<sub>2</sub> concentrations and soil diffuse flux measurements

176 Soil CO<sub>2</sub> flux was measured with an accumulation chamber near the base of the tree (generally within 5 meters, terrain  
177 permitting) at three different points and then averaged to provide a single CO<sub>2</sub> flux value to compare to the <sup>13</sup>C  
178 measurement of the corresponding tree sample. This technique is intended to provide a simple relative way to compare  
179 the CO<sub>2</sub> exposure of different trees, as a tree with high CO<sub>2</sub> flux near its base should experience consistently higher  
180 CO<sub>2</sub> concentrations than a tree with lower CO<sub>2</sub> flux. We also measured concentrations at ground level and 1.5 – 2.0  
181 m above ground level, though these were expectedly highly variable in time and location. We analyzed CO<sub>2</sub> fluxes,  
182 not concentrations, because the diffuse emissions of excess volcanic CO<sub>2</sub> through the soil, fed from a deep magma  
183 source and location-dependent on constant deep geological permeability, are highly invariant in time compared to  
184 under-canopy air concentrations. In contrast, instantaneous concentration measurements in the sub-canopy air are  
185 modulated by many factors including meteorology, respiration of vegetation and animals, uptake by plants for  
186 photosynthesis, and diurnal dynamic and slope effects. An approach of instantaneous highly variable concentration  
187 measurements is thus not representative of long-term exposure. The approach of measuring the largely invariant soil-  
188 to-atmosphere volcanic CO<sub>2</sub> fluxes is much more representative of long-term exposure, varying mostly spatially and  
189 the site-to-site differences are therefore more representative of the lifetime of exposure of the trees.

190

191 We used a custom-built soil flux chamber system which contained a LI-COR 840A non-dispersive infrared CO<sub>2</sub> sensor  
192 (LI-COR Inc., Lincoln NE, USA) to measure soil CO<sub>2</sub> flux. A custom-built cylindrical accumulation chamber of  
193 defined volume was sealed to the ground and remained connected to the LI-COR sensor. The air within the  
194 accumulation chamber was continuously recirculated through the sensor, passing through a particle filter. The sensor  
195 was calibrated before deployment and performed within specifications. We recorded cell pressure and temperature,  
196 ambient pressure, air temperature, GPS location, time stamps, location description, wind speed and direction, relative  
197 humidity, and slope, aspect, and altitude as ancillary data. In typical operation, each measurement site for flux  
198 measurements was validated for leaks (visible in the live data stream display as spikes and breaks in the CO<sub>2</sub>

199 concentration slope), and potential external disturbances were avoided (such as vehicle traffic, generators, or breathing  
200 animals and humans). Measurements were recorded in triplicate for at least 2 minutes per site. Data reduction was  
201 performed using recorded time stamps in the dataset, with conservative time margins to account for sensor response  
202 dead time, validated against consistent slope sections of increasing chamber CO<sub>2</sub>. Fluxes were computed using  
203 ancillary pressure and temperature measurements and the geometric chamber constant (chamber volume at inserted  
204 depth, tubing volume, and sensor volume). Care was taken to not disturb the soil and overlying litter inside and  
205 adjacent to the chamber.

## 206 **2.4 Leaf function measurements**

207 Chlorophyll fluorescence measurements were conducted on leaves of all three species during the field campaign to  
208 obtain information on instantaneous plant stress using an OS30p+ fluorometer (Opti-Sciences Inc., Hudson, NH,  
209 USA). Five mature leaves from each individual tree were dark adapted for at least 20 minutes to ensure complete  
210 relaxation of the photosystems. After dark adaptation, initial minimal fluorescence was recorded ( $F_0$ ) under conditions  
211 where we assume that photosystem II (PSII) was fully reduced. Immediately following the  $F_0$  measurement, a 6,000  
212  $\mu\text{mol m}^{-2} \text{s}^{-1}$  saturation pulse was delivered from an array of red LEDs at 660 nm to record maximal fluorescence  
213 emission ( $F_m$ ), when the reaction centers are assumed to be fully closed. From this, the variable fluorescence was  
214 determined as  $F_v/F_m = (F_m - F_0)/F_m$ .  $F_v/F_m$  is a widely used chlorophyll fluorescence variable used to assess the  
215 efficiency of PSII and, indirectly, plant stress (Baker and Oxborough, 2004). The five  $F_v/F_m$  measurements were  
216 averaged to provide a representative value for each individual tree. Some trees had less than five measurements due  
217 to the dark adaptation clips slipping off the leaf before measurements could be taken. Ten trees had four measurements,  
218 and another six had three measurements.

219 Chlorophyll concentration index (CCI) was measured with a MC-100 Apogee Instruments chlorophyll  
220 concentration meter (Apogee Instruments, Inc., Logan, UT, USA). CCI was converted to chlorophyll concentration  
221 ( $\mu\text{mol m}^{-2}$ ) with the generic formula derived by Parry et al., 2014. Depending on availability, between three and six  
222 leaves were measured for CCI for each tree, and then averaged to provide a single value for each tree. If leaves were  
223 not within reach, a branch was pulled down or individual leaves were shot down with a slingshot and collected.  
224 Photosynthetically active radiation was measured at each tree with a handheld quantum meter (Apogee Instruments,  
225 Logan, UT, USA) (Table S2). Stomatal conductance to water vapor,  $g_s$  ( $\text{mmol m}^{-2} \text{s}^{-1}$ ) was measured between 10:00-  
226 14:00 hours using a steady-state porometer (SC-1, Decagon Devices, Inc., Pullman, WA, USA), calibrated before use  
227 and read in manual mode. This leaf porometer was rated for humidity < 90%, and humidity was sometimes above this  
228 limit during our field work. Consequently, we have fewer stomatal conductance measurements than our other data  
229 types.

## 230 **2.5 Isotopic analysis**

231 We collected wood cores from 31 individual trees at a 1.5 m height using a 5.15 mm diameter increment borer (JIM  
232 GEM, Forestry Suppliers Inc., Jackson, MS, USA). Since no definable tree rings were apparent, we created a fine

233 powder for isotope analysis by drilling holes into dried cores using a dry ceramic drill bit (Dremel) along the outermost  
234 5 cm of wood below the bark, which was chosen to represent the most recent carbon signal for  $^{13}\text{C}$  analyses. The fine  
235 powder (200 mesh, 0.2 – 5 mg) was then mixed and a random sample was used to extract  $^{13}\text{C}/^{12}\text{C}$  ratios (to obtain  
236  $\delta^{13}\text{C}$  values against the VPDB standard), which we estimated to be representative of at least the last 2-3 years, based  
237 on analogous literature growth rate values: *O. xalapensis* and *A. acuminata* range from 0.25 - 2.5 cm/y and 0.6 - 0.9  
238 cm/y, respectively (Kappelle et al., 1996; Ortega-Pieck et al, 2011). These rates result in a 5 cm range of at least 2 and  
239 5.5 years, though the high rates were determined for very young trees under very different conditions and it is explicitly  
240 unknown in our study. Since we only sample the most recent years, no isotopic discrimination against atmospheric  
241  $^{13}\text{C}$  due to preferential diffusion and carboxylation of  $^{12}\text{C}$ , was conducted. Rather, we assume that  $\delta^{13}\text{C}$  values are  
242 representative of the relative amount of volcanic  $\text{CO}_2$  vs. atmospheric  $\text{CO}_2$  sequestered by the tree over the period of  
243 growth represented in the sample.  $\delta^{13}\text{C}$  values were determined by continuous flow dual isotope analysis using a  
244 CHNOS Elemental Analyzer and IsoPrime 100 mass spectrometer at the University of California Berkeley Center for  
245 Stable Isotope Biogeochemistry. External precision for C isotope determinations is  $\pm 0.10$  ‰. Ten  $\delta^{13}\text{C}$  measurements  
246 did not have corresponding soil  $\text{CO}_2$  flux measurements due to the flux measurements being unavailable for the final  
247 two days of sampling, and another 5 samples were from trees that showed signs of extreme stress, such as browning  
248 leaves or anomalously low fluorescence measurements. Since the purpose of our study was to explore the non-lethal  
249 effects of volcanic  $\text{CO}_2$  on trees, during analysis we excluded all trees that were observed in the field to show visible  
250 signs of stress, or that were not fully mature. After these exclusions, all remaining tree cores with co-located  $\text{CO}_2$  flux  
251 measurements were from Turrialba.

## 252 **2.6 Sulfur dioxide probability from satellite data**

253 To assess the likelihood of trees having been significantly stressed in the past by volcanic sulfur dioxide ( $\text{SO}_2$ ) from  
254 the central crater vents, we took two approaches. First, we were guided by in-situ measurements taken in the same  
255 areas by Jenkins et al. (2012), who assessed the physiological interactions of  $\text{SO}_2$  and  $\text{CO}_2$  on vegetation on the upper  
256 slopes of Turrialba and demonstrated a rapid exponential decay of  $\text{SO}_2$  away from the central vent. Second, for long-  
257 term exposure we derived the likelihood of exposure per unit area using satellite data sensitive to  $\text{SO}_2$  (Fig. 2). The  
258 Advanced Spaceborne Thermal Emission and Reflection Radiometer (ASTER), launched in December 1999 on  
259 NASA's Terra satellite, has bands sensitive to  $\text{SO}_2$  emission in the thermal infrared (TIR), at  $\sim 60$  m x 60 m spatial  
260 resolution. We initially used ASTER Surface Radiance TIR data (AST\_09T), using all ASTER observations of the  
261 target area over the entirety of the ASTER mission (October 2000 until writing in late 2017). The TIR bands were  
262 corrected for downwelling sky irradiance and converted into units of  $\text{W m}^{-2} \mu\text{m}^{-1}$ . For each observation, an absorption  
263 product is calculated by subtracting  $\text{SO}_2$ -insensitive from  $\text{SO}_2$ -sensitive bands:

$$264 \quad S^t = (b_{10} + b_{12}) - 2 \cdot b_{11} \quad (1)$$

265 Where  $S$  is the  $\text{SO}_2$  index,  $t$  is an index representing the time of acquisition,  $b_{10}$  is the radiance at band 10 (8.125 -  
266 8.475  $\mu\text{m}$ ),  $b_{11}$  is the radiance at band 11 (8.475 - 8.825  $\mu\text{m}$ ), and  $b_{12}$  is the radiance at band 12 (8.925 - 9.275  $\mu\text{m}$ ).  
267 This is similar to the method of Champion et al. (2010). The granules were then separated into day and night scenes,



268 projected onto a common grid, and then thresholded to  $S > 0.1 \text{ W m}^{-2} \mu\text{m}^{-1}$ , and converted into a probability. The  
269 output is a spatial dataset that describes the probability of an ASTER observation showing an absorption feature above  
270 a  $0.1 \text{ W m}^{-2} \mu\text{m}^{-1}$  threshold across the entirety of the ASTER observations for day or night separately. The number of  
271 scenes varies per target, but they tend to be between 200-800 observations in total, over the 17 year time period of  
272 satellite observations. However, certain permanent features, such as salt pans, show absorption features in band 11  
273 and therefore have high ratios for the algorithm used. We therefore used a second method that seeks to map transient  
274 absorption features. For this method, we subtract the median from each  $S^t$ , yielding a median deviation stack. By  
275 plotting the maximum deviations across all observations, we then get a map of transient absorption features, in our  
276 case this is mostly volcanic  $\text{SO}_2$  plumes, which map out the cumulative position of different plume observations well.  
277 To speed up processing, some of the retrieval runs were binned in order to increase the signal-to-noise ratio, since the  
278 band difference can be rather noisy.

## 279 **2.7 Modelling the anthropogenic $\text{CO}_2$ influence from inventory data**

280 We assessed the likelihood of anthropogenic  $\text{CO}_2$ , enhancements of air from San Jose, Costa Rica's capital and main  
281 industrial and population center, influencing our measurements. We used a widely applied Flexible Particle Dispersion  
282 Model (Eckhardt et al., 2017; Stohl et al., 1998, 2005; Stohl and Thomson, 1999) in a forward mode (Stohl et al.,  
283 2005), Flexpart, to simulate the downwind concentrations of  $\text{CO}_2$  in the atmosphere (e.g., Belikov et al., 2016), due  
284 to inventory-derived fossil fuel (FF) emissions in our study area for the year 2015 (Fig. 2). The National Centers for  
285 Environmental Prediction (NCEP) - Climate Forecast System Reanalysis (CFSR)  $2.5^\circ$  horizontal resolution  
286 meteorology (Saha et al., 2010b, 2010a), and 1-km Open-Source Data Inventory for Anthropogenic  $\text{CO}_2$  (ODIAC;  
287 Oda and Maksyutov, 2011) emissions for 2015 were used to drive the Flexpart model. The  $\text{CO}_2$  concentrations were  
288 generated at a 1 km spatial resolution within three vertical levels of the atmosphere (0-100, 100-300, 300-500 meters)  
289 that are possibly relevant to forest canopies in Costa Rica. However, to assess the magnitude of enhancements we only  
290 used  $\text{CO}_2$  concentrations observed within the lowest modelled level of the atmosphere, from 0-100 meters. Validation  
291 of the model with direct observations was not required because we were only interested in ensuring that anthropogenic  
292  $\text{CO}_2$  dispersed upslope from San José was not having a significant effect on our study area, we were not aiming to  
293 capture intra-canopy variability, typically at tens to hundreds of ppm variable, which is not relevant to the better  
294 mixed, distal single-digit or less ppm signal from San Jose. The actual concentration of  $\text{CO}_2$  and any biogenic influence  
295 in the modelled area was irrelevant because the spatial distribution of anthropogenic  $\text{CO}_2$  was the only factor relevant  
296 for this test. 2015 was used as a representative year for simulating the seasonal cycle of  $\text{CO}_2$  concentrations that would  
297 be present in any particular year.

## 298 **3 Results**

### 299 **3.1 Volcanic $\text{CO}_2$ emissions through the soil**

300 We measured  $\text{CO}_2$  flux emitted through the soil at 66 points over four days (Fig. 1). The first eight points were on  
301 Irazú, and the rest were located near the Ariete fault on Turrialba. Mean soil  $\text{CO}_2$  flux values over the entire sampling

302 area varied from 3 to 37 g m<sup>-2</sup> day<sup>-1</sup>, with an average of 11.6 g m<sup>-2</sup> day<sup>-1</sup> and a standard deviation of 6.6 g m<sup>-2</sup> day<sup>-1</sup>. A  
303 12-bin histogram of mean CO<sub>2</sub> flux shows a bimodal right-skewed distribution with a few distinct outliers (Fig. 3).  
304 Fluxes were generally larger on Irazú than on Turrialba. This result agrees with previous studies which showed that  
305 the north flank of Irazú has areas of extremely high degassing, whereas most of our sampling locations on Turrialba  
306 were in areas that had comparatively lower diffuse emissions (Epiard et al., 2017; Stine and Banks, 1991). We used a  
307 cumulative probability plot to identify different populations of CO<sub>2</sub> fluxes (Fig. 3) (Cardellini et al., 2003; Sinclair,  
308 1974).

309 We created an inventory-based model of anthropogenic CO<sub>2</sub> emissions from the San José urban area, parts  
310 of which are less than 15 km from some of our sampling locations (Fig. 2). Our model shows that CO<sub>2</sub> emitted from  
311 San José is blown west to south-west by prevailing winds. Our study area is directly east of San José, and as such is  
312 unaffected by anthropogenic CO<sub>2</sub> from San Jose, which is the only major urban area near Turrialba and Irazú. Since  
313 the trees sampled are spatially close to each other, they are exposed to the same regional background CO<sub>2</sub> variability.  
314 Additionally, we used ASTER data to map probabilities of SO<sub>2</sub> across Costa Rica, as a possible confounding factor.  
315 The active craters of both Turrialba and Irazú emit measurable amounts of SO<sub>2</sub>, which is reflected by the high SO<sub>2</sub>  
316 probabilities derived there (Fig. 2). Tropospheric SO<sub>2</sub> quickly converts to sulfate, a well-studied process intensified  
317 by the presence of volcanic mineral ash, plume turbulence, and a humid tropical environment (Oppenheimer et al.,  
318 1989; Eatough et al., 1994); furthermore, the bulk of the SO<sub>2</sub> emissions is carried aloft. Consequently, any remaining  
319 SO<sub>2</sub> causing acid damage effects on trees at Turrialba is limited to a narrow band of a few 100 m around the mostly  
320 quietly steaming central vent, which has been thoroughly ecologically evaluated for acid damage (Jenkins et al., 2012).  
321 D’Arcy (2018) has assessed this narrow, heavily SO<sub>2</sub>-affected area immediately surrounding the central crater vent of  
322 Turrialba, which we avoided, and our sampling sites are mostly within their control zone not considered majorly  
323 affected by SO<sub>2</sub>, but where diffuse CO<sub>2</sub> degassing dominates the excess gas phase (Epiard et al, 2017). Our study area  
324 is on the flanks of the volcano, where ASTER-derived SO<sub>2</sub> probability is minimal, and SO<sub>2</sub> influence not detectable  
325 on the ground (Jenkins et al., 2012; Champion et al., 2012). Most other volcanoes in Costa Rica emit little to no SO<sub>2</sub>  
326 on a decadal time scale, shown by the low or non-existent long-term SO<sub>2</sub> probabilities over the other volcanoes in  
327 Costa Rica (white polygons in Fig. 2).

### 328 3.2 Tree core isotopes

329 Bulk wood δ<sup>13</sup>C measurements of all samples in this study, independent of exposure, ranged from -24.03 to -28.12 ‰,  
330 with most being clustered around -26 ‰ (Fig. 4). A 5-bin histogram of all δ<sup>13</sup>C measurements shows a slightly right-  
331 skewed unimodal normal distribution, with an average of -26.37 ‰ and a standard deviation of 0.85 ‰. *A. acuminata*  
332 and *O. xalapensis* have nearly identical averages (-26.14 and -25.97 ‰, respectively), while *B. nitida* has a noticeably  
333 lighter average of -27.02 ‰. Diffuse excess CO<sub>2</sub> emissions throughout the investigation areas reflect a deep volcanic  
334 source which typically varies little in time (Epiard et al., 2017), but such diffuse emissions spatially follow geological  
335 subsurface structures (Giammanco et al., 1997). Their temporal variability therefore reflects long-term low-amplitude  
336 modulation of the volcanic heavy-δ<sup>13</sup>CO<sub>2</sub> signal, and their spatial distribution is mostly constant over tree lifetimes

337 (Aiuppa et al., 2004; Peiffer et al., 2018; Werner et al., 2014), providing a constant long-term spatial gradient of CO<sub>2</sub>  
338 exposure to the forest canopy. Our data show that in areas where CO<sub>2</sub> flux is higher, the wood cores contained  
339 progressively higher amounts of <sup>13</sup>C for two of the three species. Interestingly, our tree core δ<sup>13</sup>C showed no  
340 relationship with instantaneous stomatal conductance for any species, indicating that no stress threshold was exceeded  
341 during measurement across the sample set.

### 342 **3.3 Plant function (Fluorescence, Chlorophyll, Stomatal Conductance)**

343 Our measurements and literature data confirm that ecosystems growing in these locations are consistently exposed to  
344 excess volcanic CO<sub>2</sub>, which may impact chlorophyll fluorescence, chlorophyll concentrations, and stomatal  
345 conductance of nearby trees. After excluding visibly damaged trees, leaf fluorescence, expressed as Fv/Fm, was very  
346 high in most samples. Fv/Fm ranged from 0.75 to 0.89, with most measurements clustering between 0.8 and 0.85  
347 (Fig. 5). The fluorescence data has a left-skewed unimodal distribution. The leaf fluorescence (Fv/Fm) values for *A.*  
348 *acuminata* had a strong positive correlation with soil CO<sub>2</sub> flux ( $r^2=0.69$ ,  $p<.05$ ), while the other two species showed  
349 no correlation. No confounding factors measured were correlated with Fv/Fm for any species. In general, *B. nitida*  
350 had the highest Fv/Fm values, and *A. acuminata* and *O. xalapensis* had similar values except for a few *O. xalapensis*  
351 outliers. Chlorophyll concentration measurements were highly variable, ranging from 260 to 922 μmol m<sup>-2</sup>, with an  
352 average of 558 μmol m<sup>-2</sup> and a standard deviation of 162 μmol m<sup>-2</sup> (Fig. 6). Chlorophyll concentration had a  
353 complicated right-skewed bimodal distribution, likely due to the noticeably different averages for each species. *A.*  
354 *acuminata* and *O. xalapensis* both displayed weak correlations between chlorophyll concentration and soil CO<sub>2</sub> flux  
355 ( $r^2=0.38$  and  $r^2=0.28$ , respectively), but their trendlines were found to be almost perpendicular (Fig. 6). As CO<sub>2</sub> flux  
356 increased, *A. acuminata* showed a slight increase in chlorophyll concentration, while *O. xalapensis* had significant  
357 decreases in chlorophyll concentration. *B. nitida* individuals growing on steeper slopes had significantly lower  
358 chlorophyll concentration measurements ( $r^2=0.42$ ,  $p<.05$ ) than those on gentler slopes, a trend not expressed by either  
359 of the other two species ( $r^2=0.01$  for both), demonstrating no significant influence of slope across the majority of  
360 samples. Stomatal conductance ranged from 83.5 to 361 mmol H<sub>2</sub>O m<sup>-2</sup> s<sup>-1</sup>, with an average of 214 mmol H<sub>2</sub>O m<sup>-2</sup> s<sup>-1</sup>  
361 and a standard deviation of 73.5 mmol H<sub>2</sub>O m<sup>-2</sup> s<sup>-1</sup>. Distribution was bimodal, with peaks around 150 and 350  
362 mmol H<sub>2</sub>O m<sup>-2</sup> s<sup>-1</sup>. *A. acuminata* had a moderate positive correlation ( $r^2=0.51$ ) with soil CO<sub>2</sub> flux, but it was not  
363 statistically significant due to a lack of data points (Fig. 7) – however this is a result consistent with the observed  
364 higher chlorophyll concentration (Fig. 6). The other two species displayed no correlation with soil CO<sub>2</sub> flux. *B. nitida*  
365 had a moderate negative correlation ( $r^2=0.61$ ) with slope, similar to its correlation between chlorophyll concentration  
366 and slope.

## 367 **4 Discussion**

### 368 **4.1 Long-term plant uptake of volcanic CO<sub>2</sub>**

369 Turrialba and Irazú continuously emit CO<sub>2</sub> through their vegetated flanks, but prior to this study it was unknown if  
370 the trees growing there were utilizing this additional isotopically heavy volcanic CO<sub>2</sub>. All tree cores with

371 corresponding CO<sub>2</sub> flux measurements were from areas proximal to the Ariete fault on Turrialba, where atmospheric  
 372 and volcanic δ<sup>13</sup>C have significantly different values (-9.2 and -3.4 ‰, respectively) (Malowany et al., 2017). If the  
 373 trees assimilate volcanic CO<sub>2</sub> through their stomata, then we would expect wood δ<sup>13</sup>C to trend towards heavier values  
 374 as diffuse volcanic CO<sub>2</sub> flux increases. Studies at FACE sites have found that altering the isotopic composition of the  
 375 air by artificially adding CO<sub>2</sub> with a different carbon isotope composition than the atmosphere leads to significant  
 376 changes in the δ<sup>13</sup>C value of plant matter and tree rings growing there, leading us to expect similar effects from the  
 377 naturally added volcanic CO<sub>2</sub> (Körner, 2005). It is worth noting that the FACE CO<sub>2</sub> (δ<sup>13</sup>C = -29.7 ‰), is significantly  
 378 depleted in <sup>13</sup>C compared the atmosphere whereas volcanic CO<sub>2</sub> is enriched (δ<sup>13</sup>C = -3.4 ‰ at Turrialba) compared to  
 379 atmosphere (Körner, 2005). After excluding damaged samples and stressed trees, δ<sup>13</sup>C was strongly correlated with  
 380 soil CO<sub>2</sub> flux for both *B. nitida* and *O. xalapensis* (Fig. 4). *A. acuminata* did not have a statistically significant  
 381 correlation between soil CO<sub>2</sub> flux and δ<sup>13</sup>C, likely because it had the fewest data points and a minimal range of CO<sub>2</sub>  
 382 and δ<sup>13</sup>C values. The difference in regression slope between *B. nitida* and *O. xalapensis* (Fig. 4) may be due to  
 383 physiological differences across traits or species, and/or due to differences in exposure owing to canopy height  
 384 differences. Resolving this question would require a much larger multi-species sample size which could only be  
 385 sufficiently obtained using remote sensing methods. The strong positive correlations between CO<sub>2</sub> flux and  
 386 increasingly heavy δ<sup>13</sup>C values suggest that the trees have consistently photosynthesized with isotopically heavy  
 387 excess volcanic CO<sub>2</sub> over the last few years and are therefore growing in eCO<sub>2</sub> conditions. Assuming that most of the  
 388 variations in δ<sup>13</sup>C are caused by incorporation of heavy volcanic CO<sub>2</sub>, we can calculate the average concentration of  
 389 the mean volcanic excess CO<sub>2</sub> in the air the plants are exposed to, with a mass balance equation (Eq. 2):

$$390 \quad C_v = \frac{(\delta_b - \delta_t)}{(\delta_a - \delta_v)} C_a \quad (2)$$

391 where C<sub>v</sub> is the mean volcanic excess component of the CO<sub>2</sub> concentration in air, C<sub>a</sub> is the atmospheric “background”  
 392 (i.e., non-volcanic) CO<sub>2</sub> concentration, δ<sub>a</sub> is atmospheric δ<sup>13</sup>C, δ<sub>b</sub> is the most negative δ<sup>13</sup>C measurement for the species  
 393 being studied, δ<sub>t</sub> is the δ<sup>13</sup>C value for the tree that volcanic CO<sub>2</sub> exposure is being calculated, and δ<sub>v</sub> is δ<sup>13</sup>C of the  
 394 volcanic CO<sub>2</sub>. Background wood δ<sup>13</sup>C is the value of the point for each species with the lowest CO<sub>2</sub> flux (Fig. 4), and  
 395 the other wood δ<sup>13</sup>C measurement is any other point from the same species. Values for δ<sub>v</sub>, δ<sub>a</sub>, and C<sub>a</sub> are taken from  
 396 Malowany et al., 2017. For the tree core with the highest measured CO<sub>2</sub> flux for *O. xalapensis*, this equation yields a  
 397 mean excess volcanic CO<sub>2</sub> concentration of 115 ppm, bringing the combined mean atmospheric (including volcanic)  
 398 CO<sub>2</sub> concentration tree exposure to potentially around ~520 ppm. For *B. nitida* this equation yields 133 ppm of mean  
 399 excess volcanic CO<sub>2</sub> at the highest flux location, for a combined total mean of potentially ~538 ppm CO<sub>2</sub>. These  
 400 numbers may be on the high side as the calculation assumes that carbon isotope discrimination remains constant for  
 401 all trees within a given species, but they serve as estimate of the approximate magnitude of the average amount of  
 402 CO<sub>2</sub> that these trees are exposed to. A <sup>14</sup>C tree ring study at Mammoth Mountain found an average yearly volcanic  
 403 excess CO<sub>2</sub> exposure of 20-70 ppm over a 15-year period (Lewicki et al., 2014). Turrialba is significantly more active  
 404 than Mammoth Mountain, so trees growing in high emission areas of Turrialba may be exposed to similar or higher  
 405 amounts of CO<sub>2</sub> than the tree in the Mammoth Mountain study. Additional measurements of tree core δ<sup>13</sup>C and  
 406 associated soil CO<sub>2</sub> fluxes would help corroborate our observations, which were based on a limited number of data

407 points. Though tree ring  $^{14}\text{C}$  content in volcanically active areas has been linked to variations in volcanic  $\text{CO}_2$   
408 emissions, and comparing patterns of  $\delta^{13}\text{C}$  to  $^{14}\text{C}$  measurements for the same wood samples could provide additional  
409 confirmation of this finding (Evans et al., 2010; Lefevre et al., 2017; Lewicki et al., 2014), this additional dimension  
410 was outside the scope of this exploratory study. However, beyond such pattern confirmation, using  $^{14}\text{C}$  dating of trees  
411 exposed to naturally isotopically distinct excess  $\text{CO}_2$  is, in fact, unfortunately not a reliable method for these  
412 environments due to the well-known  $\delta^{14}\text{C}$  deficiency in trees exposed to excess volcanic  $\text{CO}_2$  which is isotopically  
413 “dead” with respect to  $^{14}\text{C}$ , creating spurious patterns that preclude dating by  $^{14}\text{C}$  (e.g., Lefevre et al., 2017; Lewicki  
414 et al., 2014).

415 Our data demonstrate that  $\text{CO}_2$  fluxes through the soil may be a representative relative measure for  $\text{eCO}_2$   
416 exposure of overlying tree canopies. Forest canopy exposure to volcanic  $\text{CO}_2$  will vary over time, as will volcanic  
417  $\text{eCO}_2$ , once emitted through the soil into the sub-canopy atmosphere, the gas experiences highly variable thermal and  
418 wind disturbances which significantly affect dispersion of  $\text{CO}_2$  on minute to minute, diurnal, and seasonal timescales  
419 (Staebler and Fitzjarrald, 2004; Thomas, 2011). These processes cause in-canopy measurements of  $\text{CO}_2$  concentration  
420 to be highly variable, making instantaneous concentration measurements in a single field campaign not representative  
421 of long-term relative magnitudes of  $\text{CO}_2$  exposure. Soil  $\text{CO}_2$  fluxes are less tied to atmospheric conditions, and are  
422 primarily externally modulated by rainfall which increases soil moisture and therefore lowers the soil’s gas  
423 permeability (Camarda et al., 2006; Viveiros et al., 2009). These fluxes can also be affected by variations in barometric  
424 pressure, but both of these factors are easily measurable and therefore can be factored in when conducting field work  
425 (Viveiros et al., 2009). Assuming the avoidance of significant rainfall and pressure spikes during sampling  
426 (measurements were conducted in the dry season and no heavy rains or significant meteorological variations in  
427 pressure occurred during field work), measuring the input of  $\text{CO}_2$  into the sub-canopy atmosphere as soil  $\text{CO}_2$  fluxes  
428 is therefore expected to better represent long-term input and exposure of tree canopies to  $\text{eCO}_2$  than direct  
429 instantaneous measurements of sub-canopy  $\text{CO}_2$  concentration. Previous studies at Turrialba have shown that local  
430 volcanic  $\text{CO}_2$  flux is relatively constant on monthly to yearly timescales (de Moor et al., 2016). Therefore, current soil  
431  $\text{CO}_2$  fluxes should give relatively accurate estimates of  $\text{CO}_2$  exposure over time. This paper corroborates that  
432 expectation by demonstrating strong spatial correlations between volcanically enhanced soil  $\text{CO}_2$  emissions with co-  
433 located stable carbon isotope signals of these emissions documented in the trees’ xylem.

434 A study at the previously mentioned Mammoth Mountain tree kill area examined the connection between  
435  $\delta^{13}\text{C}$  and volcanic  $\text{CO}_2$  fluxes, but focused on the difference between trees killed by extreme  $\text{CO}_2$  conditions and those  
436 that were still alive (Biondi and Fessenden, 1999). They concluded that the changes in  $\delta^{13}\text{C}$  that they observed were  
437 due to extreme concentrations of  $\text{CO}_2$  (soil  $\text{CO}_2$  concentrations of up to 100%) impairing the functioning of root  
438 systems, leading to closure of stomata and water stress (Biondi and Fessenden, 1999).  $\text{CO}_2$  does not inherently harm  
439 trees, but the extreme  $\text{CO}_2$  concentrations (up to 100% soil  $\text{CO}_2$ ) at the Mammoth Mountain area caused major soil  
440 acidification, which led to the tree kill (McGee and Gerlach, 1998). We have evidence that those acidification  
441 processes are not affecting our  $\delta^{13}\text{C}$  measurements, and that variations in our  $\delta^{13}\text{C}$  measurements are more likely to  
442 be caused by direct photosynthetic incorporation of isotopically heavy volcanic  $\text{CO}_2$ . Our  $\delta^{13}\text{C}$  measurements have no

443 statistically significant correlation with stomatal conductance, which suggests that our heavier  $\delta^{13}\text{C}$  measurements are  
444 not linked to stomatal closure. None of the trees included in the analysis (displayed obvious signs of stress, from water  
445 or other factors, as indicated by their high fluorescence and chlorophyll concentration values and lack of visible  
446 indicators of stress; specifically, our values of  $F_v/F_m \sim 0.8$  indicate that PSII was operating efficiently in most of the  
447 trees we measured (Baker and Oxborough, 2004). The Mammoth Mountain tree kill areas have several orders of  
448 magnitude higher  $\text{CO}_2$  fluxes (well over  $10,000 \text{ g m}^{-2} \text{ day}^{-1}$ ) than the areas we sampled (up to  $38 \text{ g m}^{-2} \text{ day}^{-1}$ ), making  
449 it much more likely that stress from soil acidification would be causing stomatal closure and affecting wood  $\delta^{13}\text{C}$   
450 measurements at Mammoth Mountain (Biondi and Fessenden, 1999; McGee and Gerlach, 1998; Werner et al., 2014).  
451 In contrast, most of the diffuse degassing at Turrialba does not lead to soil acidification or pore space saturation, as is  
452 evident in our own and others' field data (e.g., Epiard et al 2017). Thus, changes in our  $\delta^{13}\text{C}$  values are best explained  
453 by direct photosynthetic incorporation of isotopically heavy volcanic  $\text{CO}_2$ . To the best of our knowledge, this is the  
454 first time that a direct correlation between volcanic soil  $\text{CO}_2$  flux and wood  $\delta^{13}\text{C}$  has been documented. Future studies  
455 should explore this correlation further, as our findings are based on a limited sample size.

#### 456 **4.2 Short-term species response to $e\text{CO}_2$**

457 Short-term plant functional responses at the leaf level to elevated  $\text{CO}_2$  were highly species-dependent. *B. nitida* had  
458 no statistically significant functional responses to soil  $\text{CO}_2$  flux and *O. xalapensis* only had a weak negative correlation  
459 between soil  $\text{CO}_2$  flux and chlorophyll concentration (Fig. 6.). *A. acuminata*, a nitrogen fixing species, was the only  
460 species with a consistent and positive functional response to elevated  $\text{CO}_2$ , displaying a strong positive correlation  
461 with fluorescence and a weak positive correlation with chlorophyll concentration and stomatal conductance (Figs. 5-  
462 7). Previous studies which linked changes in NDVI to pre-eruptive volcanic activity on the flanks of Mt. Etna and Mt.  
463 Nyiragongo support our observation of a correlation between plant function and volcanic  $\text{CO}_2$  flux (Houlié et al.,  
464 2006; Seiler et al., 2017). This link raises the question of why only one of three species displayed strong functional  
465 responses to volcanic  $\text{CO}_2$ . The lack of response in *B. nitida* and *O. xalapensis* could be due to nitrogen limitation, a  
466 factor that would not affect *A. acuminata* due to its nitrogen fixing capability. Previous studies have found that nitrogen  
467 availability strongly controls plant responses to both naturally and artificially elevated  $\text{CO}_2$  concentrations in a variety  
468 of ecosystems, including grasslands and temperate forests (Garten et al., 2011; Hebeisen et al., 1997; Lüscher et al.,  
469 2000; Norby et al., 2010; Tognetti et al., 2000). Nitrogen limitation has been posited to be an important factor in  
470 tropical montane cloud forests and may be contributing to the lack of responses in *B. nitida* and *O. xalapensis* (Tanner  
471 et al., 1998). Due to the exploratory nature of our study, we do not have a large enough dataset to conclude that the  
472 nitrogen fixing capability of species like *A. acuminata* is the cause for its positive response to volcanically elevated  
473  $\text{CO}_2$  concentrations, as has been speculated before (Schwandner et al., 2004), but it is a possible correlation that  
474 deserves further investigation.

#### 475 **4.3 Time constraints**

476 To support these results, we further assessed the possibility of effects of time constraints on growth rates and isotopic  
477 signals, despite the compelling spatial variability of the independent variable (naturally isotopically labelled excess

478 volcanic CO<sub>2</sub>) in our study (Helle and Schleser, 2004; Verheyden et al., 2004). As tropical trees typically lack tree  
479 rings, it is difficult to directly constrain the precise time period that the data represent. However, since we sampled  
480 from the outside in, all the samples appear to at least have the most recent growth period in common. To assess how  
481 far back in time our samples could likely represent, we compared our sampled core depths to reported growth rates  
482 for the same species in similar environments. Reported growth rates for two of our species, *O. xalapensis* and *A.*  
483 *acuminata*, range from 0.25 - 2.5 cm y<sup>-1</sup> and 0.6 - 0.9 cm y<sup>-1</sup>, respectively (Kappelle et al., 1996; Ortega-Pieck et al.,  
484 2011). Given that our samples are bulk measurements of the outer 5 cm of wood, each sample would represent between  
485 2 and 5.5 years, although the conditions that these growth rates were measured in were different than in our study.  
486 Clear time constraints would be necessary for higher resolution analysis, but this need is somewhat mitigated by the  
487 continuous, long-term, and over multiple decades mostly invariant nature of diffuse volcanic CO<sub>2</sub> emissions, which is  
488 completely independent of any non-volcanic environmental influences on growth rates. By providing an upper and  
489 lower bound in the expected growth span represented in our samples, we believe that these samples represent similar  
490 time frames during the continuous exposure to excess volcanic CO<sub>2</sub> over the lifetimes of the trees sampled. Due to the  
491 continuous nature of the volcanic CO<sub>2</sub> enhancement, we are not investigating and analyzing transient events, and our  
492 results instead represent spatial variability in excess CO<sub>2</sub> availability averaged over similar time periods.

493

494 Although we do not believe our samples represent a long enough time period for long term variations in  $\delta^{13}\text{C}$  (Seuss  
495 effect) to be relevant, if it does affect our samples it would be beneficial for detection of volcanic CO<sub>2</sub> as the Seuss  
496 effect is gradually increasing the gap between atmospheric and volcanic  $\delta^{13}\text{C}$ . Since our  $\delta^{13}\text{C}$  values likely represent  
497 several years of growth, small scale temporal variations in excess volcanic CO<sub>2</sub> release are unlikely to significantly  
498 impact the results. Larger trees tend to grow slower than smaller trees, so the outer 5 cm of wood should represent a  
499 longer time period on larger trees. Thus, if temporal variations had a significant effect on our  $\delta^{13}\text{C}$  measurements, we  
500 would expect this to be represented by some correlation between DBH and  $\delta^{13}\text{C}$ , which is not present for any species  
501 studied. Three of the five *B. nitida* individuals measured were very large (150-190 cm DBH), whereas the other two  
502 are much smaller (11.5 and 15.3 cm DBH). Although the age and growth rates of these two groups of trees likely vary  
503 significantly, we found no correlation between DBH and  $\delta^{13}\text{C}$ ; though we did find a strong correlation between the  
504 completely independent diffuse excess (volcanic) CO<sub>2</sub> flux and wood  $\delta^{13}\text{C}$ . Furthermore, the relationships presented  
505 are on a per species basis to avoid complications resulting from different growth rates across species. This is important  
506 because  $\delta^{13}\text{C}$  values provide an integral value of assimilated carbon by the entire tree (not just individual leaves). The  
507 depth of tree core sample was identical for each species (the outermost part of the trunk) and we can safely assume  
508 that the volcanic CO<sub>2</sub> exposure has been consistent over the time period under investigation.

509

510 Because individual time variability of growth rates can possibly affect these signals as well, future studies that attempt  
511 to study tree ring isotopes in this context at higher resolutions will likely require stricter and more detailed time  
512 constraints and cell-level stress analysis, to average out the effects of long term variations in  $\delta^{13}\text{C}$  (Seuss effect),

513 seasonal cycles, potential short-term transient stress-induced growth rate variations, effects of water use efficiency  
514 (WUE), and potential short-term variations in CO<sub>2</sub> flux, all of which may result in time-averaged isotopic shifts over  
515 different growth periods (Helle and Schleser, 2004; Verheyden et al., 2004). We include these notes as guidance in  
516 Section 4.4: Lessons Learned for Future Studies. Despite the additional difficulty of conducting higher time resolution  
517 analysis, this type of study holds great potential for attempting to reconstruct volcanic CO<sub>2</sub> histories and to study its  
518 potential fertilization effect, due to the completely independent nature of the volcanic excess CO<sub>2</sub> supply to the sub-  
519 canopy air.

#### 520 **4.4 Lessons Learned for Future Studies**

521 This exploratory study reveals significant new potential for future studies to utilize the volcanically enhanced CO<sub>2</sub>  
522 emissions approach to study tropical ecosystem responses to eCO<sub>2</sub>—one of the largest uncertainties in climate  
523 projections. Costa Rica’s volcanoes are host to large areas of relatively undisturbed rainforest, making them ideal  
524 study areas for examining responses of ecosystems to eCO<sub>2</sub>. However, there are several challenges future studies  
525 should take into consideration if attempting to expand upon this preliminary study. Given the enormous tropical  
526 species diversity and the need to control for confounding factors, large datasets will be needed to answer these  
527 questions conclusively. One open question for example is how WUE in upper and lower canopy leaves of same and  
528 different individuals within a species may affect isotopic sequestration of CO<sub>2</sub>. Since the excess volcanic CO<sub>2</sub> is  
529 naturally isotopically labelled, this could be assessed by a much more detailed by-individual tree leaf, branch, and  
530 xylem core study coupled with long-term measurements of evapotranspiration, heat stress, and stomatal conductance,  
531 the latter of which in our study showed no significant correlation with the δ<sup>13</sup>C signal in the wood cores across spatial  
532 gradients. Field data can be difficult to acquire in these rugged and challenging environments. A remote sensing  
533 approach using airborne measurements, validated by targeted representative ground campaigns, could provide  
534 sufficiently large data sets to represent species diversity and conditions appropriately. Many of the datatypes that  
535 would be useful for this type of study can be acquired from airborne platforms, and remote sensing instruments can  
536 quickly produce the massive datasets required to provide more comprehensive answers to these questions. A recent  
537 meta-analysis showed that studies at natural CO<sub>2</sub> producing springs and FACE experiments have found similar results  
538 in a variety of plant traits, which significantly strengthens the case that volcanoes are a potentially extremely valuable  
539 resource for determining plant responses to elevated CO<sub>2</sub> concentrations (Saban et al., 2019). While the spring studies  
540 have yielded valuable results, volcanoes could offer several advantages over springs for future studies. Active  
541 volcanoes are significantly larger systems than non-volcanic springs and often feature several CO<sub>2</sub>-producing springs  
542 and also several dry gas seeps, which offers more data, more control points to compare to, greater species diversity,  
543 and greater potential for comprehensive measurements of a statistically meaningful dataset from remote sensing  
544 platforms. Due to their volcanic hazards potential, volcanoes are also more likely to already have long-term  
545 volcanological monitoring programs for CO<sub>2</sub> fluxes and ecological disturbances, which may be utilized to analyze the  
546 long-term effects of enhanced levels of CO<sub>2</sub> emissions on these volcanically active tropical ecosystems.



547 Our results also offer significant new tools for the volcanology, where reconstructing past volcano behavior through  
548 eruption histories is hampered by severe preservation gaps in the stratigraphic record. A strong link between  $\delta^{13}\text{C}$  and  
549 volcanic  $\text{CO}_2$  could be a game-changer by establishing long-term histories of volcanic  $\text{CO}_2$  emission variations. These  
550 proxy signals could be traced back in time using living and preserved dead trees, in order to fill gaps in the historical  
551 and monitoring records – a boon for volcano researchers and observatories to improve eruption prediction capabilities  
552 (Newhall et al., 2017; Pyle, 2017; Sparks et al., 2012). While variations in tree ring  $^{14}\text{C}$  content have been shown to  
553 correlate well with variations in volcanic  $\text{CO}_2$  flux (Evans et al., 2010; Lefevre et al., 2017; Lewicki and Hilley, 2014),  
554  $^{14}\text{C}$  is relatively expensive to measure, limiting the spatial and temporal coverage of data that can be acquired.  $^{13}\text{C}$  is  
555 an inexpensive alternative to  $^{14}\text{C}$  and can be measured at more laboratories, allowing for substantially more data to be  
556 acquired. Some previously mentioned studies (Lefevre et al., 2017; Pasquier-Cardin et al., 1999) have found  
557 correlations between  $^{13}\text{C}$  and  $^{14}\text{C}$  in plants that have incorporated volcanic  $\text{CO}_2$ , strengthening the potential for using  
558  $^{13}\text{C}$  in this type of study. Further development of the  $^{13}\text{C}$  approach to tracking volcanic  $\text{CO}_2$  emissions would prove  
559 beneficial to future studies attempting to use plants to study large areas and time scales of volcanic degassing.  
560 Independent validation, and calibration by wood core dendrochronology via  $^{14}\text{C}$ , tree rings, or chemical event tracers  
561 like sulfur isotopes, could significantly advance the concept of using wood carbon as archives of past degassing  
562 activity. Crucially, these tree ring archives could provide temporal records of degassing at dangerous volcanoes which  
563 have previously been poorly monitored or not monitored at all, significantly improving the accuracy of hazard  
564 assessments. Furthermore, knowledge of the short-term real-time response of leaves to diffusely emitted  $\text{eCO}_2$ , which  
565 is more likely to represent deeper processes inside volcanoes than crater-area degassing (Camarda et al., 2012), may  
566 permit the use of trees as sensors of transient changes in volcanic degassing indicative of volcanic reactivation and  
567 deep magma movement possibly leading up to eruptions (Camarda et al., 2012; Houlié et al., 2006; Pieri et al., 2016;  
568 Schwandner et al., 2017; Seiler et al., 2017; Shinohara et al., 2008; Werner et al., 2013). To the best of our knowledge,  
569 we are the first to propose utilizing the combination of short-term leaf functional responses to volcanic  $\text{CO}_2$  with long-  
570 term changes in  $\delta^{13}\text{C}$  values of wood for assessment of past and present volcanic activity in a single study.

## 571 **5 Conclusions**

572 Multiple areas of dense tropical forest on two Costa Rican active volcanoes are consistently and continuously exposed  
573 to volcanically-elevated levels of atmospheric  $\text{CO}_2$ , diffusively cold-emitted through soils into overlying forests.  
574 These isotopically heavy volcanic  $\text{CO}_2$  emissions, which are mostly invariant, not accompanied by acidic gases, and  
575 independent of processes affecting growth rates, are well correlated with increases in heavy carbon signatures in wood  
576 cores from two species of tropical trees, possibly suggesting long-term incorporation of enhanced levels of  
577 volcanically emitted  $\text{CO}_2$  into biomass. Each tree studied was co-located with a soil  $\text{CO}_2$  flux measurement and their  
578 soil  $\text{CO}_2$  flux signals vary spatially around a continuous long-term local natural excess volcanic  $\text{CO}_2$  source, which  
579 creates a local  $\text{CO}_2$  gradient within which all the sampled trees are found. The excess volcanic  $\text{CO}_2$  through local fault-  
580 bound gas seeps provides continuous exposure to all sampled trees over time scales much greater than the lifetimes of  
581 individual trees. Based on our limited exploratory measurements, confounding factors that are known to influence

582  $\delta^{13}\text{C}$  values in wood appear not to have significantly affected our measurements, indicating that the heavier wood  $\delta^{13}\text{C}$   
583 values could be caused by photosynthetic incorporation of volcanic excess  $\text{CO}_2$ . One of the three species studied (*A.*  
584 *acuminata*) has consistent positive correlations between instantaneous plant function measurements and diffuse  $\text{CO}_2$   
585 flux measurements, indicating that short-term variations in elevated  $\text{CO}_2$  emissions may measurably affect trees  
586 growing in areas of diffuse volcanic gas emissions. These observations reveal significant potential for future studies  
587 to use these areas of naturally elevated  $\text{CO}_2$  to study ecosystem responses to elevated  $\text{CO}_2$ , and to use trees as sensors  
588 of changing degassing behavior of volcanic flanks, which is indicative of deep magmatic processes.

589  
590 *Data availability.* Data can be found in Table S1 and Table S2 in the supplement or can be requested from Florian  
591 Schwandner (Florian.Schwandner@jpl.nasa.gov).

592  
593 *Author contributions.* FMS and JBF designed the study, and RRB, FMS, JBF, and ED conducted the field work and  
594 collected all samples and data with some of the equipment borrowed from GN, who helped interpret the results. TSM  
595 processed the samples for analysis. JPL conducted the  $\text{SO}_2$  analysis, wrote the related methods subsection, and helped  
596 interpret the results. VY modelled the anthropogenic  $\text{CO}_2$  emissions, wrote the related methods subsection, and helped  
597 interpret the results. CAF created the combined figure showing the  $\text{CO}_2$  and  $\text{SO}_2$  results and assisted in writing the  
598 manuscript. RRB wrote the publication, with contributions from all co-authors.

599  
600 *Competing interests.* The authors declare that they have no conflict of interest.

## 601 **Acknowledgements**

602 We are grateful for LI-COR, Inc. (Lincoln, NE, USA) providing us a loaner  $\text{CO}_2$  sensor for field work in Costa Rica.  
603 We thank Rizalina Schwandner for engineering assistance during sensor integration, OVSICORI (Observatorio  
604 Vulcanológico y Sismológico de Costa Rica, the Costa Rican volcano monitoring authority) for logistical and permit  
605 support, SINAC (Sistema Nacional de Áreas de Conservación, the Costa Rican National Parks Service) for access at  
606 Turrialba volcano, as well as Mr. Marco Antonio Otárola Rojas (Universidad Nacional de Costa Rica – ICOMVIS)  
607 for invaluable help in the field. We also thank four anonymous reviewers and the handling editor for very helpful and  
608 insightful suggestions that led us to improve the manuscript. Incidental funding is acknowledged from the S.W.  
609 Hartman Fund at Occidental College for funding R.R.B.'s field expenses, as well as the Jet Propulsion Laboratory's  
610 YIP (Year-round Internship Program) and the Jet Propulsion Laboratory Education Office for funding and support for  
611 R.R.B. F.M.S.'s UCLA contribution to this work was supported by Jet Propulsion Laboratory subcontract 1570200.  
612 Part of the research described in this paper was carried out at the Jet Propulsion Laboratory, California Institute of  
613 Technology, under a contract with the National Aeronautics and Space Administration.

614 **References**

- 615 Ainsworth, E. A. and Long, S. P.: What have we learned from 15 years of free-air CO<sub>2</sub> enrichment (FACE)? A  
616 meta-analytic review of the responses of photosynthesis, canopy properties and plant production to rising CO<sub>2</sub>, *New*  
617 *Phytol.*, 165(2), 351–372, doi:10.1111/j.1469-8137.2004.01224.x, 2005.
- 618 Aiuppa, A., Caleca, A., Federico, C., Gurrieri, S. and Valenza, M.: Diffuse degassing of carbon dioxide at Somma–  
619 Vesuvius volcanic complex (Southern Italy) and its relation with regional tectonics, *J. Volcanol. Geotherm. Res.*,  
620 133(1), 55–79, doi:10.1016/S0377-0273(03)00391-3, 2004.
- 621 Alvarado, G. E., Carr, M. J., Turrin, B. D., Swisher, C. C., Schmincke, H.-U. and Hudnut, K. W.: Recent volcanic  
622 history of Irazú volcano, Costa Rica: Alternation and mixing of two magma batches, and pervasive mixing, in  
623 *Special Paper 412: Volcanic Hazards in Central America*, vol. 412, pp. 259–276, Geological Society of America.,  
624 2006.
- 625 Baker, N. R. and Oxborough, K.: Chlorophyll Fluorescence as a Probe of Photosynthetic Productivity, in  
626 *Chlorophyll a Fluorescence*, pp. 65–82, Springer, Dordrecht., 2004.
- 627 Barquero, R., Lesage, P., Metaxian, J. P., Creusot, A. and Fernández, M.: La crisis sísmica en el volcán Irazú en  
628 1991 (Costa Rica), *Rev. Geológica América Cent.*, 0(18), doi:10.15517/rgac.v0i18.13494, 1995.
- 629 Belikov, D. A., Maksyutov, S., Yaremchuk, A., Ganshin, A., Kaminski, T., Blessing, S., Sasakawa, M., Gomez-  
630 Pelaez, A. J. and Starchenko, A.: Adjoint of the global Eulerian–Lagrangian coupled atmospheric transport model  
631 (A-GELCA v1.0): development and validation, *Geosci. Model Dev.*, 9(2), 749–764, doi:10.5194/gmd-9-749-2016,  
632 2016.
- 633 Biondi, F. and Fessenden, J. E.: Response of lodgepole pine growth to CO<sub>2</sub> degassing at Mammoth Mountain,  
634 California, *Ecol. Brooklyn*, 80(7), 2420–2426, 1999.
- 635 Burton, M. R., Sawyer, G. M. and Granieri, D.: Deep Carbon Emissions from Volcanoes, *Rev. Mineral. Geochem.*,  
636 75(1), 323–354, doi:10.2138/rmg.2013.75.11, 2013.
- 637 Camarda, M., Gurrieri, S. and Valenza, M.: CO<sub>2</sub> flux measurements in volcanic areas using the dynamic  
638 concentration method: Influence of soil permeability, *J. Geophys. Res. Solid Earth*, 111(B5), B05202,  
639 doi:10.1029/2005JB003898, 2006.
- 640 Camarda, M., De Gregorio, S. and Gurrieri, S.: Magma-ascent processes during 2005–2009 at Mt Etna inferred by  
641 soil CO<sub>2</sub> emissions in peripheral areas of the volcano, *Chem. Geol.*, 330–331, 218–227,  
642 doi:10.1016/j.chemgeo.2012.08.024, 2012.
- 643 Champion, R., Salerno, G. G., Coheur, P.-F., Hurtmans, D., Clarisse, L., Kazahaya, K., Burton, M., Caltabiano, T.,  
644 Clerbaux, C. and Bernard, A.: Measuring volcanic degassing of SO<sub>2</sub> in the lower troposphere with ASTER band  
645 ratios, *J. Volcanol. Geotherm. Res.*, 194(1–3), 42–54, doi:10.1016/j.jvolgeores.2010.04.010, 2010.
- 646 Cardellini, C., Chiodini, G. and Frondini, F.: Application of stochastic simulation to CO<sub>2</sub> flux from soil: Mapping  
647 and quantification of gas release, *J. Geophys. Res. Solid Earth*, 108(B9), 2425, doi:10.1029/2002JB002165, 2003.
- 648 Cawse-Nicholson, K., Fisher, J. B., Famiglietti, C. A., Braverman, A., Schwandner, F. M., Lewicki, J. L.,  
649 Townsend, P. A., Schimel, D. S., Pavlick, R., Bormann, K. J., Ferraz, A., Kang, E. L., Ma, P., Bogue, R. R.,  
650 Youmans, T. and Pieri, D. C.: Ecosystem responses to elevated CO<sub>2</sub> using airborne remote sensing at Mammoth  
651 Mountain, California, *Biogeosciences*, 15(24), 7403–7418, doi:https://doi.org/10.5194/bg-15-7403-2018, 2018.
- 652 Chiodini, G., Cioni, R., Guidi, M., Raco, B. and Marini, L.: Soil CO<sub>2</sub> flux measurements in volcanic and geothermal  
653 areas, *Appl. Geochem.*, 13(5), 543–552, doi:10.1016/S0883-2927(97)00076-0, 1998.

- 654 Cook, A. C., Hainsworth, L. J., Sorey, M. L., Evans, W. C. and Southon, J. R.: Radiocarbon studies of plant leaves  
655 and tree rings from Mammoth Mountain, CA: a long-term record of magmatic CO<sub>2</sub> release, *Chem. Geol.*, 177(1),  
656 117–131, 2001.
- 657 Cox, P., Pearson, D., Booth, B., Friedlingstein, P., Huntingford, C., Jones, C. and Luke, M.: Sensitivity of  
658 tropical carbon to climate change constrained by carbon dioxide variability., 2013.
- 659 Delmelle, P. and Stix, J.: *Volcanic Gases*, edited by H. Sigurdsson, B. Houghton, H. Rymer, J. Stix, and S. McNutt,  
660 Encyclopedia Volcanoes, 1417, 1999.
- 661 Dietrich, V. J., Fiebig, J., Chiodini, G. and Schwandner, F. M.: Fluid Geochemistry of the Hydrothermal System, in  
662 Nisyros Volcano, edited by V. J. Dietrich, E. Lagios, and O. Bachmann, p. 339, Springer, Berlin., 2016.
- 663 Eckhardt, S., Cassiani, M., Evangeliou, N., Sollum, E., Pisso, I. and Stohl, A.: Source–receptor matrix calculation  
664 for deposited mass with the Lagrangian particle dispersion model FLEXPART v10.2 in backward mode, *Geosci.*  
665 *Model Dev.* Katlenburg-Lindau, 10(12), 4605–4618, doi:<http://dx.doi.org/10.5194/gmd-10-4605-2017>, 2017.
- 666 Epiard, M., Avaré, G., de Moor, J. M., Martínez Cruz, M., Barrantes Castillo, G. and Bakkar, H.: Relationship  
667 between Diffuse CO<sub>2</sub> Degassing and Volcanic Activity. Case Study of the Poás, Irazú, and Turrialba Volcanoes,  
668 Costa Rica, *Front. Earth Sci.*, 5, doi:10.3389/feart.2017.00071, 2017.
- 669 Evans, W. C., Bergfeld, D., McGeehin, J. P., King, J. C. and Heasler, H.: Tree-ring <sup>14</sup>C links seismic swarm to CO<sub>2</sub>  
670 spike at Yellowstone, USA, *Geology*, 38(12), 1075–1078, 2010.
- 671 Farrar, C. D., Sorey, M. L., Evans, W. C., Howle, J. F., Kerr, B. D., Kennedy, B. M., King, C.-Y. and Southon, J.  
672 R.: Forest-killing diffuse CO<sub>2</sub> emission at Mammoth Mountain as a sign of magmatic unrest, *Nature*, 376(6542),  
673 675–678, doi:10.1038/376675a0, 1995.
- 674 Friedlingstein, P., Meinshausen, M., Arora, V. K., Jones, C. D., Anav, A., Liddicoat, S. K. and Knutti, R.:  
675 Uncertainties in CMIP5 Climate Projections due to Carbon Cycle Feedbacks, *J. Clim.*, 27(2), 511–526,  
676 doi:10.1175/JCLI-D-12-00579.1, 2013.
- 677 Garten, C. T., Iversen, C. M. and Norby, R. J.: Litterfall <sup>15</sup>N abundance indicates declining soil nitrogen availability  
678 in a free-air CO<sub>2</sub> enrichment experiment, *Ecology*, 92(1), 133–139, doi:10.1890/10-0293.1, 2011.
- 679 Global Volcanism Program: *Volcanoes of the World*, v. 4.6.5, edited by E. Venzke, Smithsonian Inst.,  
680 doi:<https://dx.doi.org/10.5479/si.GVP.VOTW4-2013>, 2013.
- 681 Gregory, J. M., Jones, C. D., Cadule, P. and Friedlingstein, P.: Quantifying Carbon Cycle Feedbacks, *J. Clim.*,  
682 22(19), 5232–5250, doi:10.1175/2009JCLI2949.1, 2009.
- 683 Hattenschwiler, S., Miglietta, F., Raschi, A. and Körner, C.: Thirty years of in situ tree growth under elevated CO<sub>2</sub>: a  
684 model for future forest responses?, *Glob. Change Biol.*, 3(5), 463–471, doi:10.1046/j.1365-2486.1997.00105.x,  
685 1997.
- 686 Hebeisen, T., Lüscher, A., Zanetti, S., Fischer, B., Hartwig, U., Frehner, M., Hendrey, G., Blum, H. and Nösberger\*,  
687 J.: Growth response of *Trifolium repens* L. and *Lolium perenne* L. as monocultures and bi-species mixture to free air  
688 CO<sub>2</sub> enrichment and management, *Glob. Change Biol.*, 3(2), 149–160, doi:10.1046/j.1365-2486.1997.00073.x,  
689 1997.
- 690 Helle, G. and Schleser, G. H.: Beyond CO<sub>2</sub>-fixation by Rubisco – an interpretation of <sup>13</sup>C/<sup>12</sup>C variations in tree rings  
691 from novel intra-seasonal studies on broad-leaf trees, *Plant Cell Environ.*, 27(3), 367–380, doi:10.1111/j.0016-  
692 8025.2003.01159.x, 2004.

- 693 Houlié, N., Komorowski, J. C., de Michele, M., Kasereka, M. and Ciraba, H.: Early detection of eruptive dykes  
694 revealed by normalized difference vegetation index (NDVI) on Mt. Etna and Mt. Nyiragongo, *Earth Planet. Sci.*  
695 *Lett.*, 246(3), 231–240, doi:10.1016/j.epsl.2006.03.039, 2006.
- 696 Kappelle, M., Geuze, T., Leal, M. E. and Cleef, A. M.: Successional age and forest structure in a Costa Rican upper  
697 montane *Quercus* forest, *J. Trop. Ecol.*, 12(05), 681–698, doi:10.1017/S0266467400009871, 1996.
- 698 Kauwe, M. G. D., Keenan, T. F., Medlyn, B. E., Prentice, I. C. and Terrer, C.: Satellite based estimates  
699 underestimate the effect of CO<sub>2</sub> fertilization on net primary productivity, *Nat. Clim. Change*, 6(10), 892,  
700 doi:10.1038/nclimate3105, 2016.
- 701 Keeling, C. D.: The Carbon Dioxide Cycle: Reservoir Models to Depict the Exchange of Atmospheric Carbon  
702 Dioxide with the Oceans and Land Plants, in *Chemistry of the Lower Atmosphere*, edited by S. I. Rasool, pp. 251–  
703 329, Springer US, Boston, MA., 1973.
- 704 Körner, C.: Carbon Flux and Growth in Mature Deciduous Forest Trees Exposed to Elevated CO<sub>2</sub>, *Science*,  
705 309(5739), 1360–1362, doi:10.1126/science.1113977, 2005.
- 706 Körner, C. and Miglietta, F.: Long term effects of naturally elevated CO<sub>2</sub> on mediterranean grassland and forest  
707 trees, *Oecologia*, 99(3), 343–351, doi:10.1007/BF00627748, 1994.
- 708 Lefevre, J.-C., Gillot, P.-Y., Cardellini, C., Gresse, M., Lesage, L., Chiodini, G. and Oberlin, C.: Use of the  
709 Radiocarbon Activity Deficit in Vegetation as a Sensor of CO<sub>2</sub> Soil Degassing: Example from La Solfatara (Naples,  
710 Southern Italy), *Radiocarbon*, 1–12, doi:10.1017/RDC.2017.76, 2017.
- 711 Leigh, E. G., Losos, E. C. and Research, N. B. of E.: Tropical forest diversity and dynamism : findings from a large-  
712 scale network, Chicago, Ill. ; London : The University of Chicago Press. [online] Available from:  
713 <http://trove.nla.gov.au/version/12851528> (Accessed 25 September 2017), 2004.
- 714 Lewicki, J. L. and Hilley, G. E.: Multi-scale observations of the variability of magmatic CO<sub>2</sub> emissions, Mammoth  
715 Mountain, CA, USA, *J. Volcanol. Geotherm. Res.*, 284(Supplement C), 1–15, doi:10.1016/j.jvolgeores.2014.07.011,  
716 2014.
- 717 Lewicki, J. L., Hilley, G. E., Shelly, D. R., King, J. C., McGeehin, J. P., Mangan, M. and Evans, W. C.: Crustal  
718 migration of CO<sub>2</sub>-rich magmatic fluids recorded by tree-ring radiocarbon and seismicity at Mammoth Mountain,  
719 CA, USA, *Earth Planet. Sci. Lett.*, 390, 52–58, doi:10.1016/j.epsl.2013.12.035, 2014.
- 720 Lüscher, A., Hartwig, U. A., Suter, D. and Nösberger, J.: Direct evidence that symbiotic N<sub>2</sub> fixation in fertile  
721 grassland is an important trait for a strong response of plants to elevated atmospheric CO<sub>2</sub>, *Glob. Change Biol.*, 6(6),  
722 655–662, doi:10.1046/j.1365-2486.2000.00345.x, 2000.
- 723 Malowany, K. S., Stix, J., de Moor, J. M., Chu, K., Lacrampe-Couloume, G. and Sherwood Lollar, B.: Carbon  
724 isotope systematics of Turrialba volcano, Costa Rica, using a portable cavity ring-down spectrometer, *Geochem.*  
725 *Geophys. Geosystems*, 18(7), 2769–2784, doi:10.1002/2017GC006856, 2017.
- 726 Martini, F., Tassi, F., Vaselli, O., Del Potro, R., Martinez, M., del Laat, R. V. and Fernandez, E.: Geophysical,  
727 geochemical and geodetical signals of reawakening at Turrialba volcano (Costa Rica) after almost 150 years of  
728 quiescence, *J. Volcanol. Geotherm. Res.*, 198(3–4), 416–432, doi:10.1016/j.jvolgeores.2010.09.021, 2010.
- 729 Mason, E., Edmonds, M. and Turchyn, A. V.: Remobilization of crustal carbon may dominate volcanic arc  
730 emissions, *Science*, 357(6348), 290–294, 2017.
- 731 McGee, K. A. and Gerlach, T. M.: Annual cycle of magmatic CO<sub>2</sub> in a tree-kill soil at Mammoth Mountain,  
732 California: Implications for soil acidification, *Geology*, 26(5), 463–466, 1998.

- 733 de Moor, J. M., Aiuppa, A., Avarð, G., Wehrmann, H., Dunbar, N., Muller, C., Tamburello, G., Giudice, G., Liuzzo,  
734 M., Moretti, R., Conde, V. and Galle, B.: Turmoil at Turrialba Volcano (Costa Rica): Degassing and eruptive  
735 processes inferred from high-frequency gas monitoring, *J. Geophys. Res. Solid Earth*, 121(8), 2016JB013150,  
736 doi:10.1002/2016JB013150, 2016.
- 737 Newhall, C. G., Costa, F., Ratdompurbo, A., Venezky, D. Y., Widiwijayanti, C., Win, N. T. Z., Tan, K. and  
738 Fajiculay, E.: WOVOdat – An online, growing library of worldwide volcanic unrest, *J. Volcanol. Geotherm. Res.*,  
739 345, 184–199, doi:10.1016/j.jvolgeores.2017.08.003, 2017.
- 740 Nicholson, E.: *Volcanology: An Introduction*, Larsen and Keller Education., 2017.
- 741 Norby, R. J., Warren, J. M., Iversen, C. M., Medlyn, B. E. and McMurtrie, R. E.: CO<sub>2</sub> enhancement of forest  
742 productivity constrained by limited nitrogen availability, *Proc. Natl. Acad. Sci.*, 107(45), 19368–19373,  
743 doi:10.1073/pnas.1006463107, 2010.
- 744 Norby, R. J., De Kauwe, M. G., Domingues, T. F., Duursma, R. A., Ellsworth, D. S., Goll, D. S., Lapola, D. M.,  
745 Luus, K. A., MacKenzie, A. R., Medlyn, B. E., Pavlick, R., Rammig, A., Smith, B., Thomas, R., Thonicke, K.,  
746 Walker, A. P., Yang, X. and Zaehle, S.: Model–data synthesis for the next generation of forest free-air CO<sub>2</sub>  
747 enrichment (FACE) experiments, *New Phytol.*, 209(1), 17–28, doi:10.1111/nph.13593, 2016.
- 748 Norman, E. M.: *Buddlejaceae (Flora Neotropica Monograph No. 81)*, The New York Botanical Garden Press., 2000.
- 749 Oda, T. and Maksyutov, S.: A very high-resolution (1 km×1 km) global fossil fuel CO<sub>2</sub> emission inventory derived  
750 using a point source database and satellite observations of nighttime lights, *Atmos Chem Phys*, 11(2), 543–556,  
751 doi:10.5194/acp-11-543-2011, 2011.
- 752 Ortega-Pieck, A., López-Barrera, F., Ramírez-Marcial, N. and García-Franco, J. G.: Early seedling establishment of  
753 two tropical montane cloud forest tree species: The role of native and exotic grasses, *For. Ecol. Manag.*, 261(7),  
754 1336–1343, doi:10.1016/j.foreco.2011.01.013, 2011.
- 755 Paoletti, E., Seufert, G., Della Rocca, G. and Thomsen, H.: Photosynthetic responses to elevated CO<sub>2</sub> and O<sub>3</sub> in  
756 *Quercus ilex* leaves at a natural CO<sub>2</sub> spring, *Environ. Pollut.*, 147(3), 516–524, doi:10.1016/j.envpol.2006.08.039,  
757 2007.
- 758 Parry, C., Blonquist, J. M. and Bugbee, B.: In situ measurement of leaf chlorophyll concentration: analysis of the  
759 optical/absolute relationship, *Plant Cell Environ.*, 37(11), 2508–2520, doi:10.1111/pce.12324, 2014.
- 760 Pasquier-Cardin, A., Allard, P., Ferreira, T., Hatte, C., Coutinho, R., Fontugne, M. and Jaudon, M.: Magma-derived  
761 CO<sub>2</sub> emissions recorded in 14C and 13C content of plants growing in Furnas caldera, Azores, *J. Volcanol.*  
762 *Geotherm. Res.*, 92(1), 195–207, doi:10.1016/S0377-0273(99)00076-1, 1999.
- 763 Peiffer, L., Wanner, C. and Lewicki, J. L.: Unraveling the dynamics of magmatic CO<sub>2</sub> degassing at Mammoth  
764 Mountain, California, *Earth Planet. Sci. Lett.*, 484, 318–328, doi:10.1016/j.epsl.2017.12.038, 2018.
- 765 Pérez, N., Hernandez, P., Padilla, G., Nolasco, D., Barrancos, J., Melián, G., Padrón, E., Dionis, S., Calvo, D. and  
766 Rodr'iguez, F.: Global CO<sub>2</sub> emission from volcanic lakes., 2011.
- 767 Pieri, D., Schwandner, F. M., Realmuto, V. J., Lundgren, P. R., Hook, S., Anderson, K., Buongiorno, M. F., Diaz, J.  
768 A., Gillespie, A., Miklius, A., Mothes, P., Mougini-Mark, P., Pallister, M., Poland, M., Palgar, L. L., Pata, F.,  
769 Pritchard, M., Self, S., Sigmundsson, F., de Silva, S. and Webley, P.: Enabling a global perspective for deterministic  
770 modeling of volcanic unrest, [online] Available from:  
771 [https://hyspiri.jpl.nasa.gov/downloads/RFI2\\_HyspIRI\\_related\\_160517/RFI2\\_final\\_PieriDavidC-final-rev.pdf](https://hyspiri.jpl.nasa.gov/downloads/RFI2_HyspIRI_related_160517/RFI2_final_PieriDavidC-final-rev.pdf)  
772 (Accessed 20 February 2018), 2016.

- 773 Pinkard, E. A., Beadle, C. L., Mendham, D. S., Carter, J. and Glen, M.: Determining photosynthetic responses of  
774 forest species to elevated CO<sub>2</sub>: alternatives to FACE, *For. Ecol. Manag.*, 260(8), 1251–1261, 2010.
- 775 Pyle, D. M.: What Can We Learn from Records of Past Eruptions to Better Prepare for the Future?, in SpringerLink,  
776 pp. 1–18, Springer, Berlin, Heidelberg., 2017.
- 777 Quintana-Ascencio, P. F., Ramírez-Marcial, N., González-Espinosa, M. and Martínez-Ic6, M.: Sapling survival and  
778 growth of coniferous and broad-leaved trees in successional highland habitats in Mexico, *Appl. Veg. Sci.*, 7(1), 81–  
779 88, 2004.
- 780 Rizzo, A. L., Di Piazza, A., de Moor, J. M., Alvarado, G. E., Avar, G., Carapezza, M. L. and Mora, M. M.:  
781 Eruptive activity at Turrialba volcano (Costa Rica): Inferences from <sup>3</sup>He/<sup>4</sup>He in fumarole gases and chemistry of the  
782 products ejected during 2014 and 2015, *Geochem. Geophys. Geosystems*, 17(11), 4478–4494,  
783 doi:10.1002/2016GC006525, 2016.
- 784 Saban, J. M., Chapman, M. A. and Taylor, G.: FACE facts hold for multiple generations; Evidence from natural CO  
785 2 springs, *Glob. Change Biol.*, 25(1), 1–11, doi:10.1111/gcb.14437, 2019.
- 786 Saha, S., Moorthi, S., Pan, H.-L., Wu, X., Wang, J., Nadiga, S., Tripp, P., Kistler, R., Woollen, J., Behringer, D.,  
787 Liu, H., Stokes, D., Grumbine, R., Gayno, G., Wang, J., Hou, Y.-T., Chuang, H., Juang, H.-M. H., Sela, J., Iredell,  
788 M., Treadon, R., Kleist, D., Van Delst, P., Keyser, D., Derber, J., Ek, M., Meng, J., Wei, H., Yang, R., Lord, S., van  
789 den Dool, H., Kumar, A., Wang, W., Long, C., Chelliah, M., Xue, Y., Huang, B., Schemm, J.-K., Ebisuzaki, W.,  
790 Lin, R., Xie, P., Chen, M., Zhou, S., Higgins, W., Zou, C.-Z., Liu, Q., Chen, Y., Han, Y., Cucurull, L., Reynolds, R.  
791 W., Rutledge, G. and Goldberg, M.: NCEP Climate Forecast System Reanalysis (CFSR) 6-hourly Products, January  
792 1979 to December 2010, *Bull. Am. Meteorol. Soc.*, 91(8), 1015–1058, doi:10.5065/D69K487J, 2010a.
- 793 Saha, S., Moorthi, S., Pan, H.-L., Wu, X., Wang, J., Nadiga, S., Tripp, P., Kistler, R., Woollen, J., Behringer, D.,  
794 Liu, H., Stokes, D., Grumbine, R., Gayno, G., Wang, J., Hou, Y.-T., Chuang, H., Juang, H.-M. H., Sela, J., Iredell,  
795 M., Treadon, R., Kleist, D., Van Delst, P., Keyser, D., Derber, J., Ek, M., Meng, J., Wei, H., Yang, R., Lord, S., van  
796 den Dool, H., Kumar, A., Wang, W., Long, C., Chelliah, M., Xue, Y., Huang, B., Schemm, J.-K., Ebisuzaki, W.,  
797 Lin, R., Xie, P., Chen, M., Zhou, S., Higgins, W., Zou, C.-Z., Liu, Q., Chen, Y., Han, Y., Cucurull, L., Reynolds, R.  
798 W., Rutledge, G. and Goldberg, M.: The NCEP Climate Forecast System Reanalysis, *Bull. Am. Meteorol. Soc.*,  
799 91(8), 1015–1058, doi:10.1175/2010BAMS3001.1, 2010b.
- 800 Saurer, M., Cherubini, P., Bonani, G. and Siegwolf, R.: Tracing carbon uptake from a natural CO<sub>2</sub> spring into tree  
801 rings: an isotope approach, *Tree Physiol.*, 23(14), 997–1004, doi:10.1093/treephys/23.14.997, 2003.
- 802 Schimel, D., Stephens, B. B. and Fisher, J. B.: Effect of increasing CO<sub>2</sub> on the terrestrial carbon cycle, *Proc. Natl.*  
803 *Acad. Sci.*, 112(2), 436–441, doi:10.1073/pnas.1407302112, 2015.
- 804 Schwandner, F. M., Seward, T. M., Gize, A. P., Hall, P. A. and Dietrich, V. J.: Diffuse emission of organic trace  
805 gases from the flank and crater of a quiescent active volcano (Vulcano, Aeolian Islands, Italy), *J. Geophys. Res.*  
806 *Atmospheres*, 109(D4), D04301, doi:10.1029/2003JD003890, 2004.
- 807 Schwandner, F. M., Gunson, M. R., Miller, C. E., Carn, S. A., Eldering, A., Krings, T., Verhulst, K. R., Schimel, D.  
808 S., Nguyen, H. M., Crisp, D., O’Dell, C. W., Osterman, G. B., Iraci, L. T. and Podolske, J. R.: Spaceborne detection  
809 of localized carbon dioxide sources, *Science*, 358(6360), eaam5782, doi:10.1126/science.aam5782, 2017.
- 810 Seiler, R., Kirchner, J. W., Krusic, P. J., Tognetti, R., Houli6, N., Andronico, D., Cullotta, S., Egli, M., D’Arrigo, R.  
811 and Cherubini, P.: Insensitivity of Tree-Ring Growth to Temperature and Precipitation Sharpens the Puzzle of  
812 Enhanced Pre-Eruption NDVI on Mt. Etna (Italy), *PLOS ONE*, 12(1), e0169297,  
813 doi:10.1371/journal.pone.0169297, 2017.

- 814 Sharma, S. and Williams, D.: Carbon and oxygen isotope analysis of leaf biomass reveals contrasting photosynthetic  
815 responses to elevated CO<sub>2</sub> near geologic vents in Yellowstone National Park, *Biogeosciences*, 6(1), 25,  
816 doi:10.5194/bg-6-25-2009, 2009.
- 817 Shinohara, H., Aiuppa, A., Giudice, G., Gurrieri, S. and Liuzzo, M.: Variation of H<sub>2</sub>O/CO<sub>2</sub> and CO<sub>2</sub>/SO<sub>2</sub> ratios of  
818 volcanic gases discharged by continuous degassing of Mount Etna volcano, Italy, *J. Geophys. Res. Solid Earth*,  
819 113(B9), doi:10.1029/2007JB005185, 2008.
- 820 Sinclair, A. J.: Selection of threshold values in geochemical data using probability graphs, *J. Geochem. Explor.*,  
821 3(2), 129–149, doi:10.1016/0375-6742(74)90030-2, 1974.
- 822 Sorey, M. L., Evans, W. C., Kennedy, B. M., Farrar, C. D., Hainsworth, L. J. and Hausback, B.: Carbon dioxide and  
823 helium emissions from a reservoir of magmatic gas beneath Mammoth Mountain, California, *J. Geophys. Res. Solid*  
824 *Earth*, 103(B7), 15303–15323, doi:10.1029/98JB01389, 1998.
- 825 Sparks, R. S. J., Biggs, J. and Neuberg, J. W.: Monitoring Volcanoes, *Science*, 335(6074), 1310–1311,  
826 doi:10.1126/science.1219485, 2012.
- 827 Staebler, R. M. and Fitzjarrald, D. R.: Observing subcanopy CO<sub>2</sub> advection, *Agric. For. Meteorol.*, 122(3–4), 139–  
828 156, doi:10.1016/j.agrformet.2003.09.011, 2004.
- 829 Stine, C. M. and Banks, N. G.: Costa Rica Volcano Profile, USGS Numbered Series, U.S. Geological Survey.  
830 [online] Available from: <https://pubs.er.usgs.gov/publication/ofr91591>, 1991.
- 831 Stohl, A. and Thomson, D. J.: A Density Correction for Lagrangian Particle Dispersion Models, *Bound.-Layer*  
832 *Meteorol.*, 90(1), 155–167, doi:10.1023/A:1001741110696, 1999.
- 833 Stohl, A., Hittenberger, M. and Wotawa, G.: Validation of the Lagrangian particle dispersion model FLEXPART  
834 against large-scale tracer experiment data, *Atmos. Environ.*, 32(24), 4245–4264, 1998.
- 835 Stohl, A., Forster, C., Frank, A., Seibert, P. and Wotawa, G.: Technical note: The Lagrangian particle dispersion  
836 model FLEXPART version 6.2, *Atmospheric Chem. Phys.*, 5(9), 2461–2474, doi:[https://doi.org/10.5194/acp-5-](https://doi.org/10.5194/acp-5-2461-2005)  
837 2461-2005, 2005.
- 838 Symonds, R. B., Gerlach, T. M. and Reed, M. H.: Magmatic gas scrubbing: implications for volcano monitoring, *J.*  
839 *Volcanol. Geotherm. Res.*, 108(1), 303–341, doi:10.1016/S0377-0273(00)00292-4, 2001.
- 840 Tanner, E. V. J., Vitousek, P. M. and Cuevas, E.: Experimental Investigation of Nutrient Limitation of Forest  
841 Growth on Wet Tropical Mountains, *Ecology*, 79(1), 10–22, doi:10.1890/0012-  
842 9658(1998)079[0010:EIONLO]2.0.CO;2, 1998.
- 843 Tercek, M. T., Al-Niemi, T. S. and Stout, R. G.: Plants Exposed to High Levels of Carbon Dioxide in Yellowstone  
844 National Park: A Glimpse into the Future?, *Yellowstone Sci.*, 16(1), 12–19, 2008.
- 845 Thomas, C. K.: Variability of Sub-Canopy Flow, Temperature, and Horizontal Advection in Moderately Complex  
846 Terrain, *Bound.-Layer Meteorol.*, 139(1), 61–81, doi:10.1007/s10546-010-9578-9, 2011.
- 847 Tognetti, R., Cherubini, P. and Innes, J. L.: Comparative stem-growth rates of Mediterranean trees under  
848 background and naturally enhanced ambient CO<sub>2</sub> concentrations, *New Phytol.*, 146(1), 59–74, doi:10.1046/j.1469-  
849 8137.2000.00620.x, 2000.
- 850 Townsend, A. R., Cleveland, C. C., Houlton, B. Z., Alden, C. B. and White, J. W.: Multi-element regulation of the  
851 tropical forest carbon cycle, *Front. Ecol. Environ.*, 9(1), 9–17, doi:10.1890/100047, 2011.



- 852 Verheyden, A., Helle, G., Schleser, G. H., Dehairs, F., Beeckman, H. and Koedam, N.: Annual cyclicality in high-  
853 resolution stable carbon and oxygen isotope ratios in the wood of the mangrove tree *Rhizophora mucronata*, *Plant*  
854 *Cell Environ.*, 27(12), 1525–1536, doi:10.1111/j.1365-3040.2004.01258.x, 2004.
- 855 Viveiros, F., Ferreira, T., Silva, C. and Gaspar, J.: Meteorological factors controlling soil gases and indoor CO<sub>2</sub>  
856 concentration: A permanent risk in degassing areas, *Sci. Total Environ.*, 407(4), 1362–1372,  
857 doi:10.1016/j.scitotenv.2008.10.009, 2009.
- 858 Vodnik, D., Thomalla, A., Ferlan, M., Levanič, T., Eler, K., Ogrinc, N., Wittmann, C. and Pfanz, H.: Atmospheric  
859 and geogenic CO<sub>2</sub> within the crown and root of spruce (*Picea abies* L. Karst.) growing in a mofette area, *Atmos.*  
860 *Environ.*, 182, 286–295, doi:10.1016/j.atmosenv.2018.03.043, 2018.
- 861 Weng, C., Bush, M. B. and Chepstow-Lusty, A. J.: Holocene changes of Andean alder(*Alnus acuminata*) in highland  
862 Ecuador and Peru, *J. Quat. Sci.*, 19(7), 685–691, doi:10.1002/jqs.882, 2004.
- 863 Werner, C., Kelly, P. J., Doukas, M., Lopez, T., Pfeffer, M., McGimsey, R. and Neal, C.: Degassing of CO<sub>2</sub>, SO<sub>2</sub>,  
864 and H<sub>2</sub>S associated with the 2009 eruption of Redoubt Volcano, Alaska, *J. Volcanol. Geotherm. Res.*, 259, 270–284,  
865 doi:10.1016/j.jvolgeores.2012.04.012, 2013.
- 866 Werner, C., Bergfeld, D., Farrar, C. D., Doukas, M. P., Kelly, P. J. and Kern, C.: Decadal-scale variability of diffuse  
867 CO<sub>2</sub> emissions and seismicity revealed from long-term monitoring (1995–2013) at Mammoth Mountain, California,  
868 USA, *J. Volcanol. Geotherm. Res.*, 289, 51–63, doi:10.1016/j.jvolgeores.2014.10.020, 2014.
- 869 Williams-Jones, G., Stix, J., Heiligmann, M., Charland, A., Lollar, B. S., Arner, N., Garzón, G. V., Barquero, J. and  
870 Fernandez, E.: A model of diffuse degassing at three subduction-related volcanoes, *Bull. Volcanol.*, 62(2), 130–142,  
871 2000.
- 872
- 873

874  
875

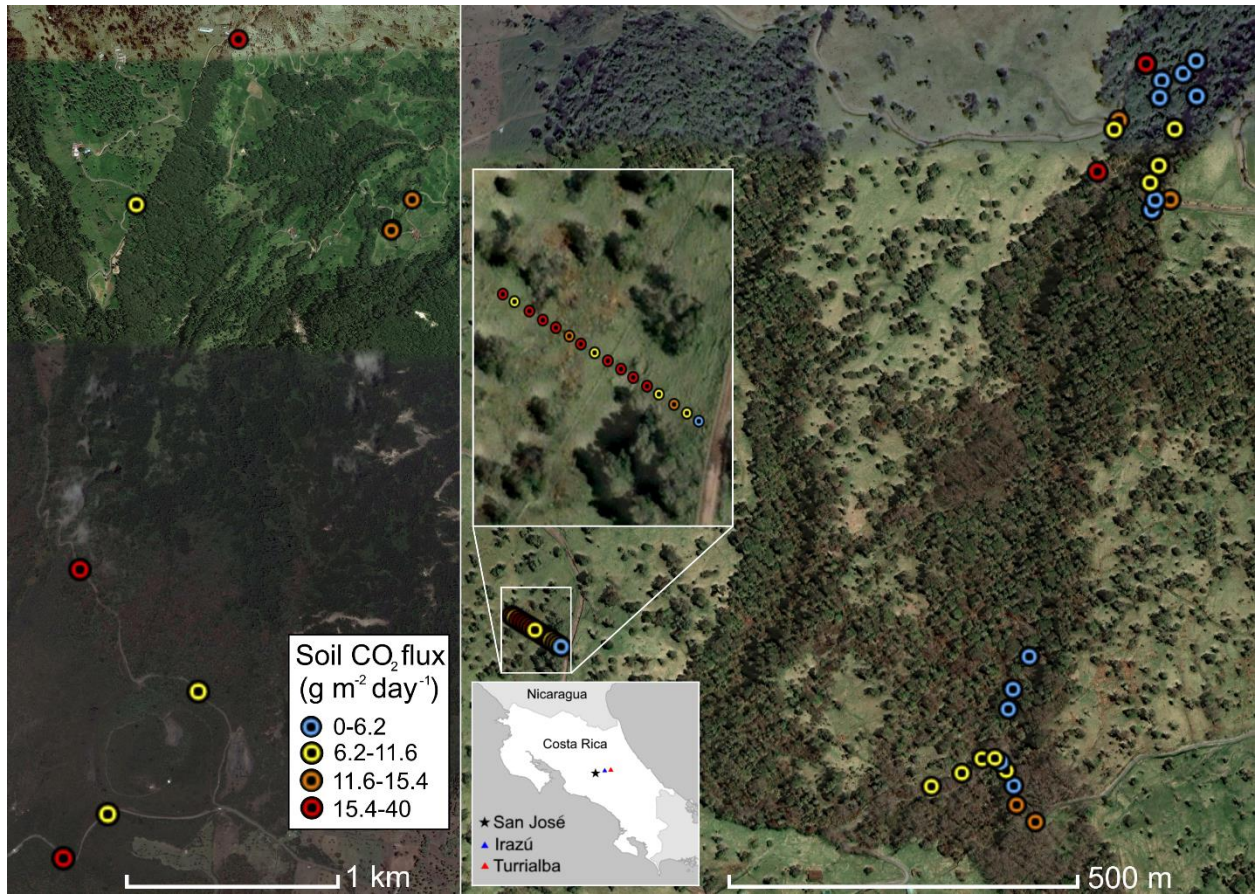


**Fig. 1: Overview of measurement locations in two old-growth forests on the upper flanks of two active volcanoes in Costa Rica, Turrialba and Irazú. Distribution of mean soil CO<sub>2</sub> flux across north flank of Irazú (left) and south flank of Turrialba (right). Colors of dots correspond to flux populations (see Fig. 3).**

876

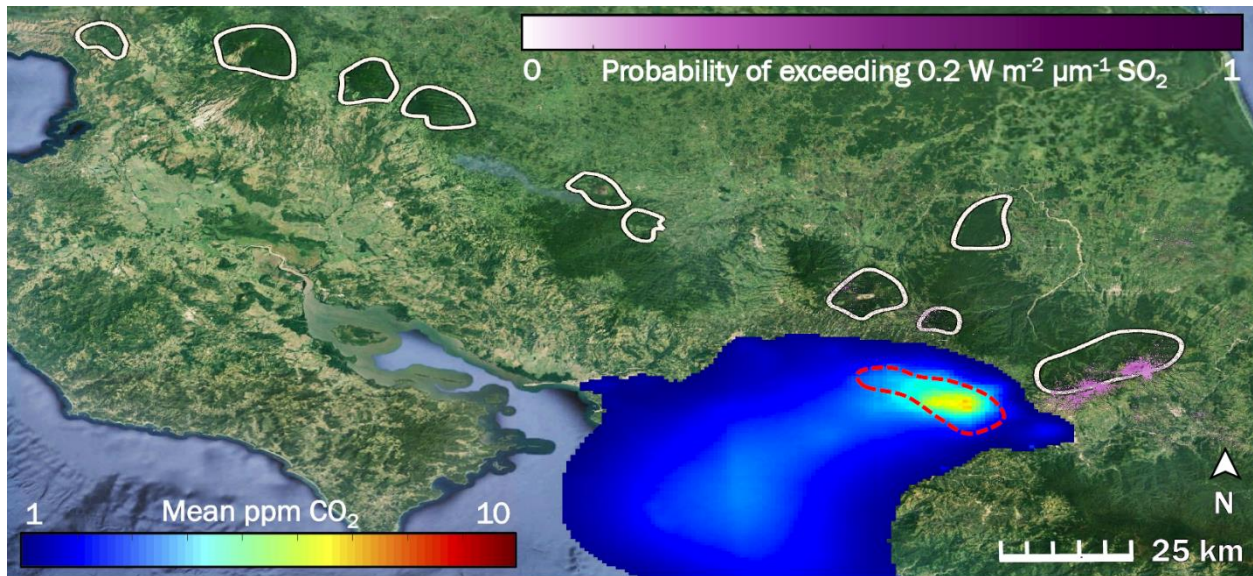


**Fig. 2:** The influence of two potentially confounding gases on our study area (right hand white polygon) in Costa Rica is low to non-existent: anthropogenic  $\text{CO}_2$  from San José (blue to red color scale), and volcanic  $\text{SO}_2$  (purple color scale). White polygons are drawn around locations of the forested active volcanic edifices in Costa Rica. The dashed red line indicates the rough border of the San José urban area. Prevailing winds throughout the year consistently blow all anthropogenic  $\text{CO}_2$  away from our study area and from all other white polygons.

877  
878  
879

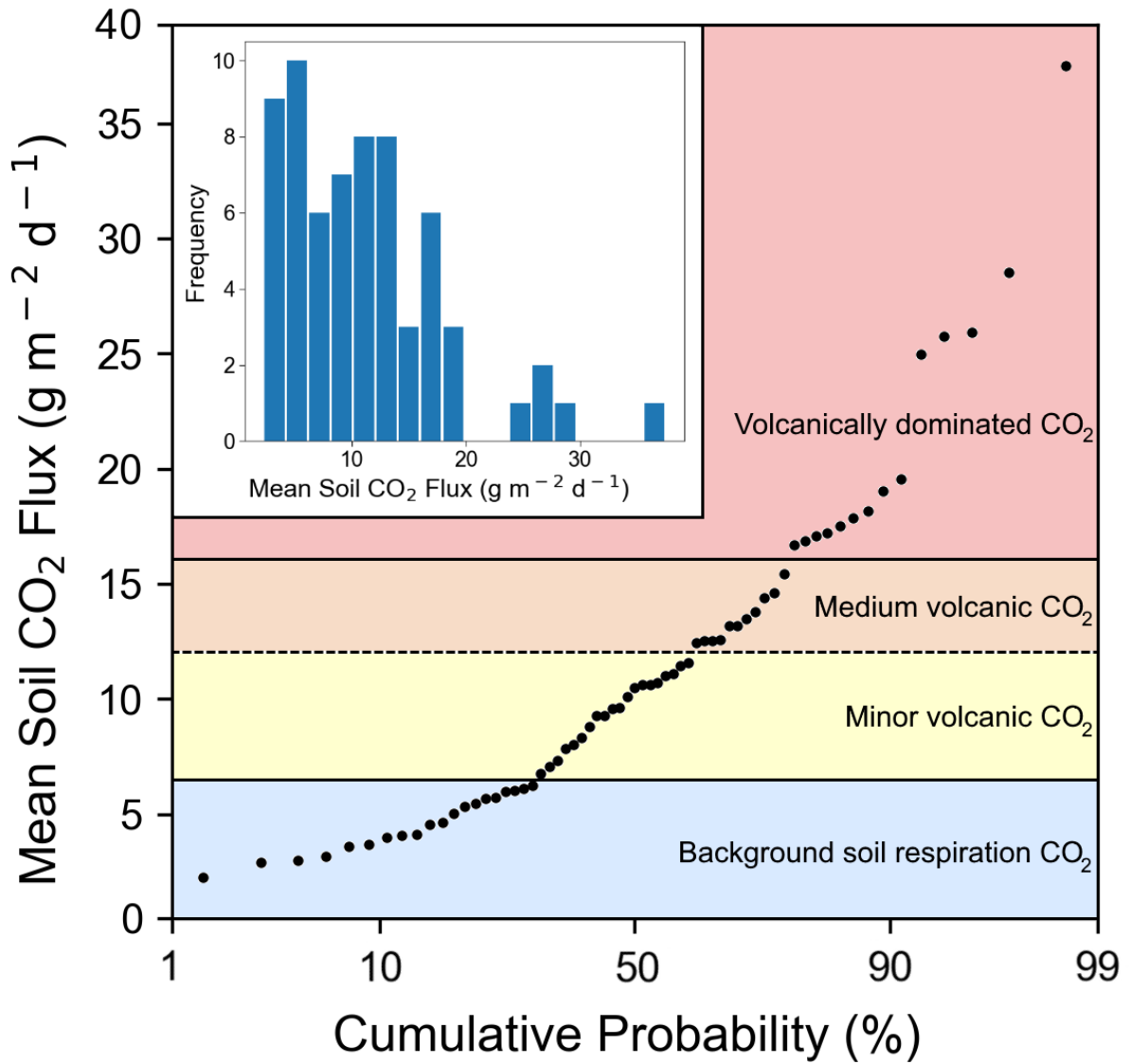


**Fig 3: Soil CO<sub>2</sub> flux into the sub-canopy air of forests on the Turrialba-Irazú volcanic complex is pervasively and significantly influenced by a deep volcanic gas source. At least four different overlapping populations of soil CO<sub>2</sub> flux were identified, using a cumulative probability plot, where inflection points indicate population boundaries (Sinclair 1974). 69% of sampling locations (45 total) are exposed to varying degrees of volcanically derived elevated CO<sub>2</sub>. Populations are color-coded based on the same color scale as Fig. 1.**

880  
881  
882

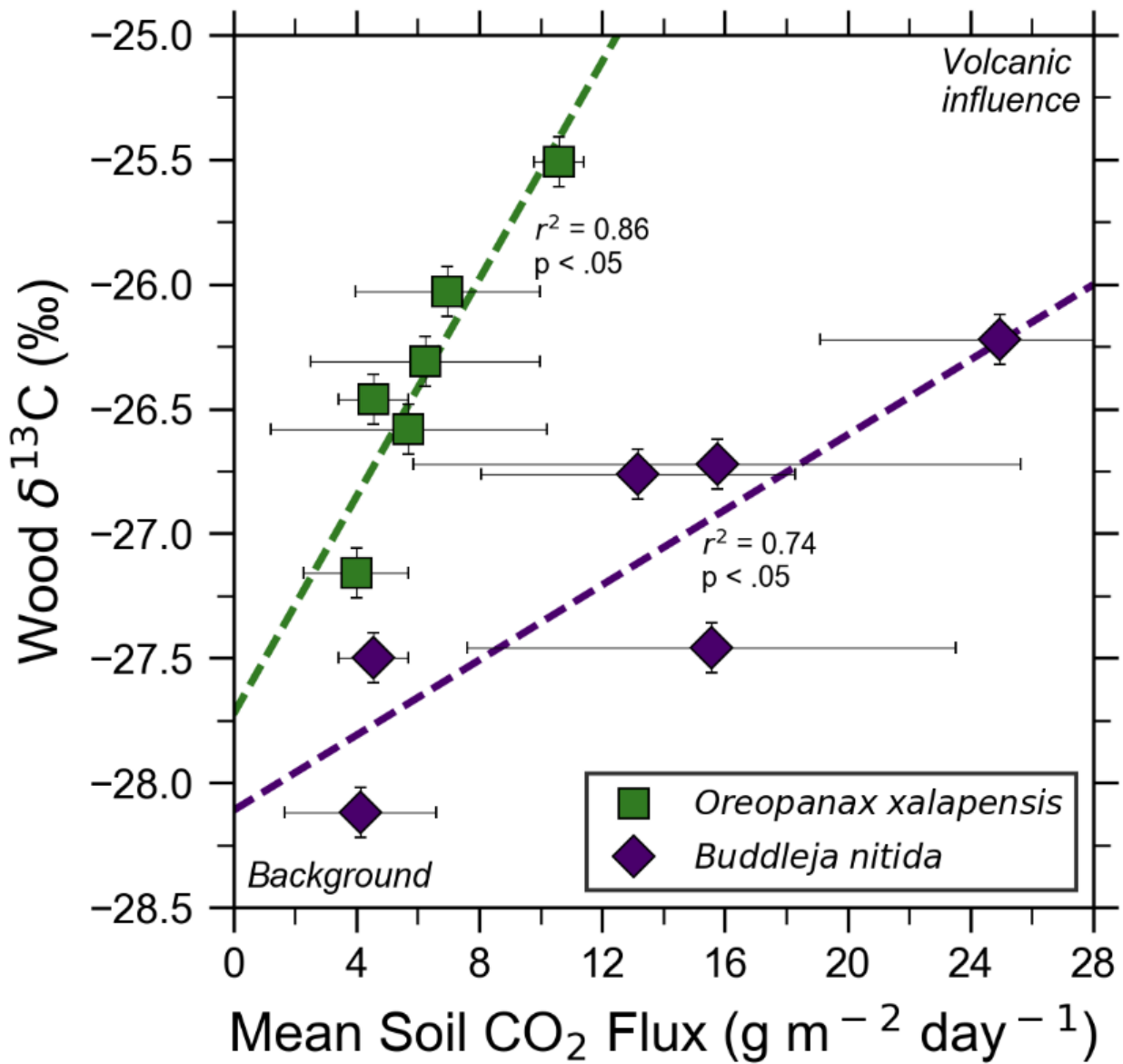
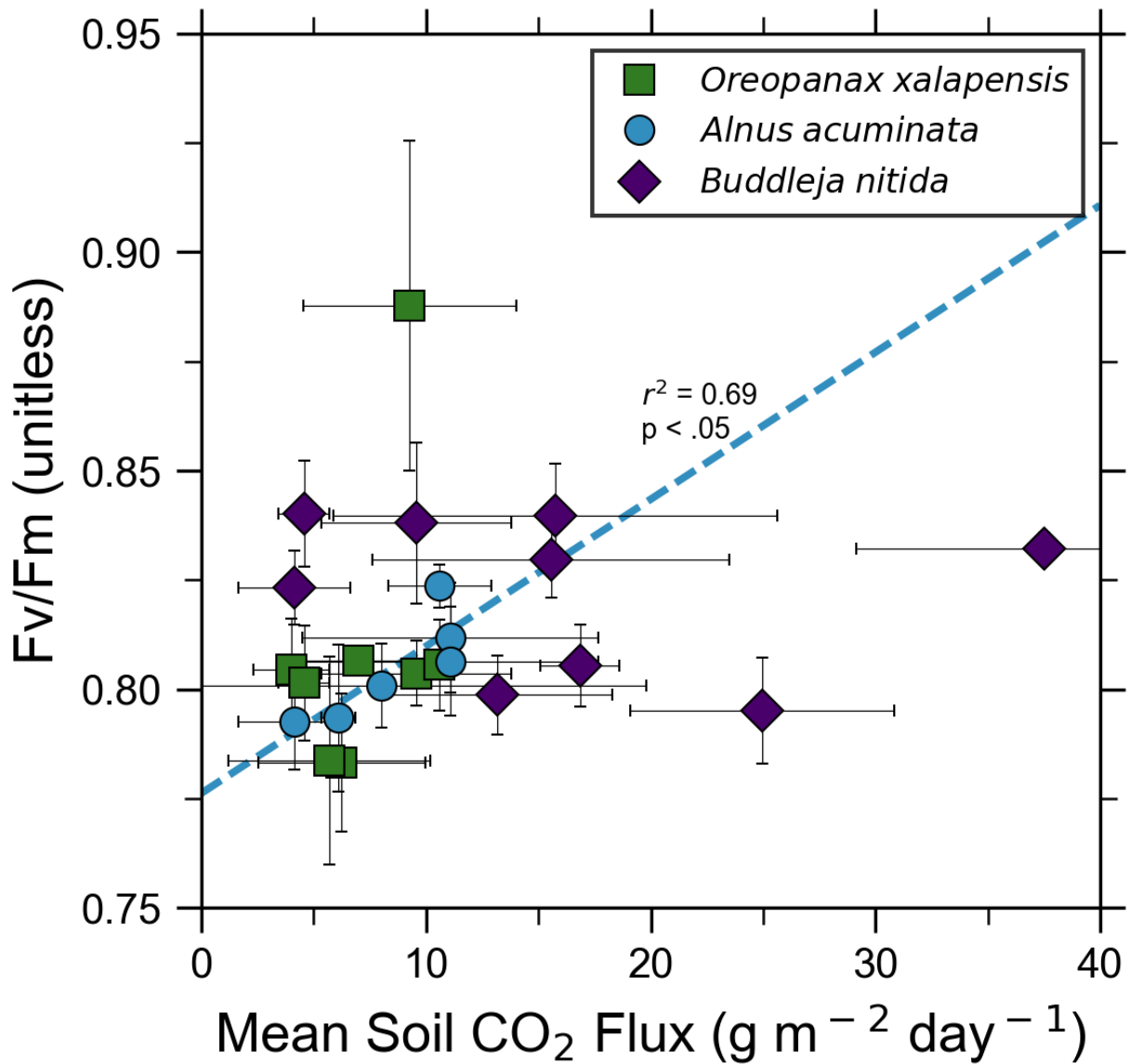
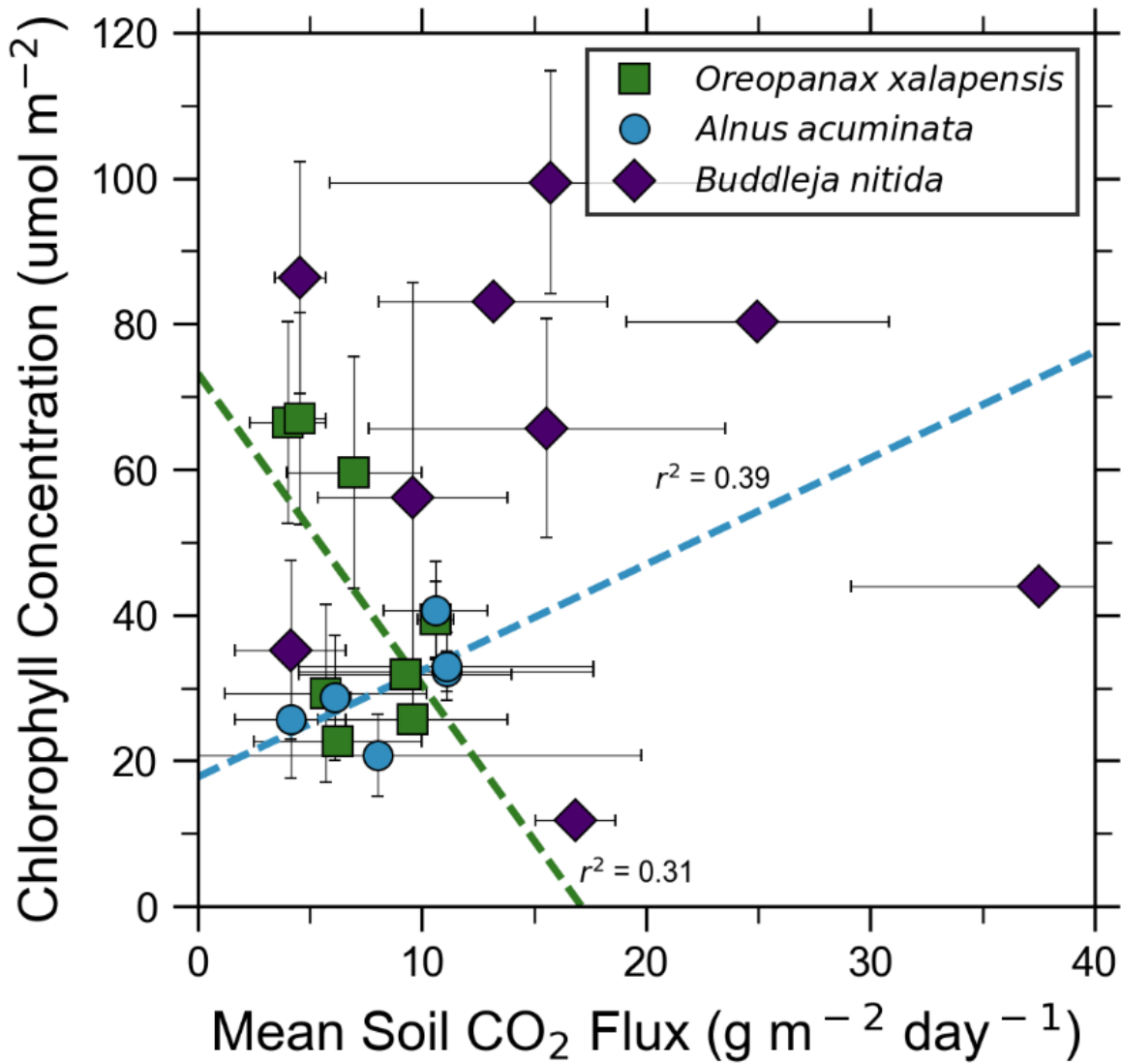


Fig 4: Bulk wood  $\delta^{13}\text{C}$  of trees on Costa Rica's Turrialba volcano shows strong correlations with increasing volcanic  $\text{CO}_2$  flux for two species, *O. xalapensis* and *B. nitida*, indicating long-term photosynthetic incorporation of isotopically heavy volcanic  $\text{CO}_2$ . Stable carbon isotope ratio ( $\delta^{13}\text{C}$ ) of wood cores are plotted against soil  $\text{CO}_2$  flux measured immediately adjacent to the tree that the core sample was taken from. Background and volcanic influence labels apply to both axes – higher  $\text{CO}_2$  flux and heavier (less negative)  $\delta^{13}\text{C}$  values are both characteristic of volcanic  $\text{CO}_2$  emissions.



**Fig. 5:** Photosynthetic activity of some tree species in old-growth forests on the upper flanks of two active volcanoes in Costa Rica, Turrialba and Irazú, may show short-term response to volcanically elevated CO<sub>2</sub>. Leaf fluorescence (Fv/Fm) and soil CO<sub>2</sub> flux were strongly correlated for *A. acuminata*, but not for other species.

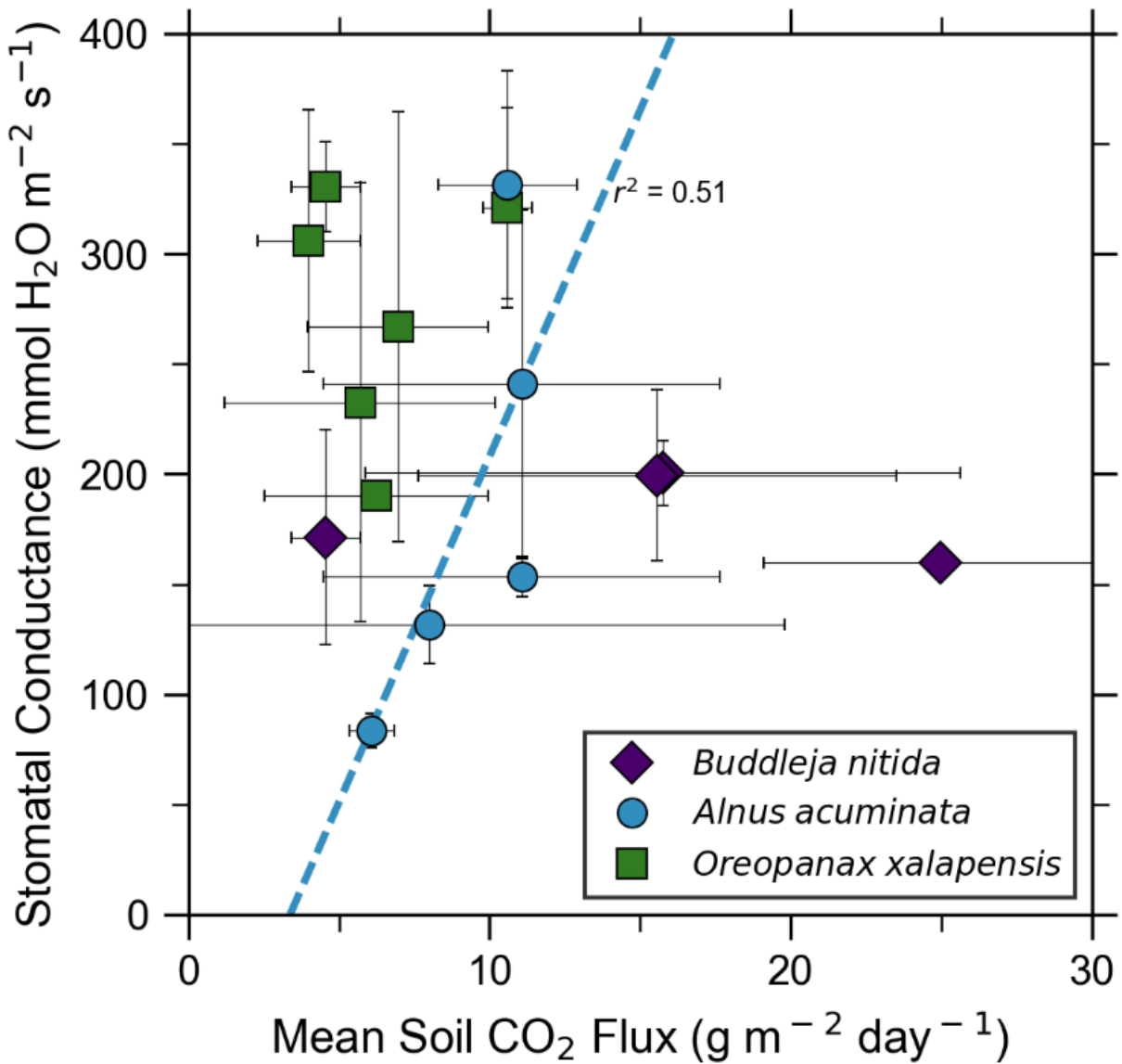


884

**Fig. 6:** Some tree species in old-growth forests on the upper flanks of two active volcanoes in Costa Rica, Turrialba and Irazú, may express their short-term response to volcanically elevated CO<sub>2</sub> by producing more chlorophyll. A species that showed strong short-term response (*A. Acuminata*, Fig. 5) also shows a positive correlation between chlorophyll concentration and mean soil CO<sub>2</sub> flux.

885

886



887

**Fig. 7:** Leaf stomatal conductance of a tree species that strongly responds to volcanically elevated CO<sub>2</sub> (Figs. 5, 6) has positive correlations with volcanic CO<sub>2</sub> flux, consistent with increased gas-exchange.

888